UPPSALA
UNIVERSITET

Digital Comprehensive Summaries of Uppsala Dissertations from the Faculty of Science and Technology 702

Charged Higgs Bosons at the ATLAS Experiment and Beyond

ELIAS CONIAVITIS

ACTA
UNIVERSITATIS
UPSALIENSIS
UPPSALA
2010

ISSN 1651-6214
ISBN 978-91-554-7693-9
urn:nbn:se:uu:diva-111576

Dissertation presented at Uppsala University to be publicly examined in Polhemssalen, Ångströmslaboratoriet, Lägerhyddsvägen 1, Uppsala, Friday, February 12, 2010 at 10:15 for the degree of Doctor of Philosophy. The examination will be conducted in English.

Abstract

Coniavitis, E. 2010. Charged Higgs Bosons at the ATLAS Experiment and Beyond. Acta Universitatis Upsaliensis. *Digital Comprehensive Summaries of Uppsala Dissertations from the Faculty of Science and Technology* 702. 61 pp. Uppsala. ISBN 978-91-554-7693-9.

In the ATLAS experiment at the Large Hadron Collider (LHC) at CERN, direct searches for the elusive Higgs boson will be conducted, as well as for physics beyond the Standard Model. The charged Higgs boson ($H^{\pm}$) is interesting both as a part of the Higgs sector, and as a clear sign of new physics. This thesis focuses on $H^{\pm}$ searches, with $H^{\pm}$ production in top-antitop pair events, and in particular the $bW^{\pm}$ $bH^{\pm}$, $H^{\pm}\rightarrow\tau_{\mathrm{had}}\nu$, $W^{\pm}\rightarrow qq$ channel. Its potential was investigated as part of a larger study of the expected performance of the entire ATLAS experiment. Full simulation of the ATLAS detector and trigger was used, and all dominant systematics considered. It was shown to be the most promising $H^{\pm}$ discovery channel for $m_{H^{\pm}}<m_t$.

As hadronic τ decays are important for $H^{\pm}$ searches, their correct identification is critical. Possibilities of improving tau-jet identification in pile-up and top-antitop pair events were investigated. Redundant or even performance-reducing variables in the default likelihood identification were identified, as were new variables showing discriminatory power. This allows for increased rejection of QCD jets in these environments, and higher robustness of the method.

Before any physics studies, a commissioned and well-understood detector is required. The Lorentz angle of the ATLAS Semi-Conductor Tracker (SCT) barrel was measured using 2008 cosmic-ray data. It is an important observable for the performance of several detector aspects. Potential sources of systematics were investigated and evaluated. The Lorentz angle in the SCT barrel was measured as $\theta_L = 3.93 \pm 0.03(stat) \pm 0.10(syst)$ degrees, agreeing with the model prediction.

The Compact Linear Collider (CLIC) is a proposed successor to the LHC. The potential for charged and heavy neutral Higgs bosons at CLIC was investigated, in terms of both discovery and precision measurement of parameters like tanβ or the Higgs masses, up to and beyond 1 TeV, which would be challenging at the LHC

Keywords: particle physics, Standard Model, beyond the Standard Model, supersymmetry, MSSM, Higgs physics, charged Higgs boson, LHC, ATLAS, ATLAS Semi-Conductor Tracker, SCT, tau lepton, Lorentz angle, CLIC

Elias Coniavitis, High Energy Physics, Box 535, Uppsala University, SE-75121 Uppsala, Sweden

ISSN 1651-6214
ISBN 978-91-554-7693-9
urn:nbn:se:uu:diva-111576 (http://urn.kb.se/resolve?urn=urn:nbn:se:uu:diva-111576)

Till Thomas, Lotta och Amanda

Cover Image: Display of a 900 GeV collision event in ATLAS
(run 141749, recorded December 6, 2009), showing tracks in the Inner
Detector system. http://www.atlas.ch/photos/events-collision.html

List of Papers

This thesis is based on the following papers, which are referred to in the text by their Roman numerals.

I Coniavitis, E., Okamoto, A., Tanaka R.
Lorentz Angle and Cluster Width Studies for the ATLAS SCT
ATL-COM-INDET-2009-039 (2009)

II Coniavitis, E., Flechl, M.
ATLAS Tau Identification in High-Multiplicity Environments
ATL-PHYS-INT-2009-106 (2009)

III The ATLAS Collaboration
Charged Higgs Boson Searches
Expected Performance of the ATLAS Experiment: Detector, Trigger and Physics, CERN-OPEN-2008-020 (2008), pp 1451-1479

IV Coniavitis, E., Ferrari, A.
Pair production of heavy MSSM charged and neutral Higgs bosons in multi-TeV e^+ e^- collisions at the Compact Linear Collider.
Physical Review D 75, 015004 (2007)

List of papers not included in this thesis:

1. Coniavitis, E.
   ChargedHiggsView: a tool for ATLAS charged Higgs boson searches
   ATL-PHYS-INT-2008-001 (2008)

2. Rozen, Y., Vickey, T., Behar Harpaz, S., Coniavitis, E., Flechl, M., Gross, E., Mellado, B., Mohn, B., Vitells, O., Wu, S.L.
   A Control Sample for $t\bar{t}$+jets Backgrounds with One or More τ Leptons in the Final State
   ATL-PHYS-INT-2009-078 (2009)

3. Assamagan, K., Behar, S., Coniavitis, E., Dufour, M -A., Ehrich, T., Flechl, M., Gross, E., Lane, J., Mohn, B., Mohrdieck-Möck, S., Potter, C., Robertson, S., Rozen, Y., Sopczak, A., Talby, M., Vachon, B., Vickey, T., Vitells, O., Yang, U.K., Zaidan, R.
   ATLAS Charged Higgs Boson Searches
   ATL-PHYS-INT-2008-046 (2008)

4. Coniavitis, E., Ferrari, A.
   Charged Higgs bosons at the Compact Linear Collider
   PoS(CHARGED2008)022 (2009)

5. Coniavitis, E. (for the ATLAS Collaboration)
   Light Charged Higgs Searches in the Hadronic Mode with ATLAS
   PoS(CHARGED2008)036 (2009)

Contents

1. Introduction

Ἐτεῇ δὲ ἄτομα καὶ κενόν
– Democritus

The question *"What is matter?"* is one of those great questions which keeps returning in the history of Science, and which has guided many great minds to historical new discoveries. Today, the field of Science that deals with this question is Particle Physics, and its tools are on one hand elaborate equations, and on the other enormous accelerators and detectors, the largest scientific instruments created by mankind. The most ambitious of these, the Large Hadron Collider (LHC) [1] at CERN, saw its first collisions only weeks before this thesis was submitted and will soon start delivering its first physics results.

While enormous progress has been made in the exploration and understanding of matter's smallest known components, culminating in the formulation and repeated experimental verification of the Standard Model of Particle Physics, several important questions still remain, which the LHC seeks to address. One of these pertains to the elusive Higgs boson [2, 3], the particle responsible for giving mass to all others, and the only particle predicted by the Standard Model not yet discovered. The second major question is a lot wider, and asks what lies beyond the Standard Model: there are several reasons to believe that the Standard Model is not a complete description of all fundamental particles and their interactions, most importantly since it does not contain a description of gravity.

At the cross-roads of these two large questions lies the main topic of this thesis, the experimental search, with the ATLAS [4] detector at the LHC, for the charged Higgs boson – a Higgs boson not predicted by the Standard Model, but required by a large number of physics theories beyond it, such as Supersymmetry.

At the same time, this thesis also details work on different aspects of the huge effort of preparation for LHC collisions data at the ATLAS detector. It thus deals with components all along the chain that a detected event would follow – from the silicon strip tracker and its commissioning (Paper I), through the process of identification of tau-jets and its refinement (Paper II), to then conclude with (simulated) data analysis and the expected reach of ATLAS for charged Higgs bosons lighter than the top quark (Paper III). Finally it also takes a look at what lies beyond the LHC, and the potential for discoveries of

charged and neutral Higgs bosons at a proposed future linear multi-TeV e^+e^- collider, the Compact Linear Collider (CLIC) [5] (Paper IV).

Chapter 2 briefly describes the theoretical framework of this thesis, covering both the Standard Model and the most dominant theory for physics beyond it – Supersymmetry. The phenomenology of charged and heavy neutral Higgs bosons in the context of the Minimal Supersymmetric Extension of the Standard Model (MSSM) is touched upon, with a short discussion of their production mechanisms and possible decays, as well as the current experimental constraints.

Chapter 3 describes the accelerators and the detectors of relevance for this thesis. Both the LHC and CLIC are presented, while most of the chapter is devoted to a description of the ATLAS detector, with special emphasis on the Semi-Conductor Tracker (SCT) and its commissioning with cosmic-ray data. A discussion on the methodology for determination of the ATLAS physics potential in simulation studies is also included in this chapter.

Chapter 4 is devoted to a description of the methods for reconstruction and identification of hadronically decaying τ leptons in ATLAS – important, amongst others, for the detection of Charged Higgs bosons.

Chapter 5 gives a short summary of the papers included in this thesis, Chapter 6 presents some conclusions and outlook, and Chapter 7 is a summary in Swedish.

2. The Standard Model and Beyond

2.1 The Standard Model

Developed in the 1960s and 1970s, the Standard Model (SM) [6, 7, 8] of particle physics is a theory describing the fundamental building blocks of matter and their interactions through the strong, weak and electromagnetic forces. An impressively successful theory, its predictions are to to this date in agreement with all experimental results, to a remarkable degree of precision.

According to the Standard Model, matter is made up of particles with half-integer spin called fermions, which can be of two categories – leptons and quarks, organised into three generations, as illustrated in Table 2.1. Besides matter, the Standard Model also includes anti-matter: to each particle corresponds an anti-particle, which has the opposite charge, but otherwise identical quantum numbers and mass.

Each quark generation consists of one up-type quark (u,c,t) and one down-type quark (d,s,b). Up-type quarks have an electric charge of $+\frac{2}{3}$ and down-type quarks have an electric charge of $-\frac{1}{3}$. In addition to their electric charge, quarks also have colour, the conserved charge of the strong interaction. A quark may be of either red, blue or green colour charge. Anti-quarks have anti-color charge.

Free particles are required to have a total colour charge of zero, which is obtained when green, red and blue charges are combined or when a color and its corresponding anti-color charge are combined. This means that it is impossible to observe isolated quarks or anti-quarks outside composite objects such as nucleons.

Leptons on the other hand do not have color charge, and therefore do not interact strongly. Only the heavy leptons (electron, muon and tau and their

Table 2.1: *Quark and Lepton Generations*

Generation	Quarks	Leptons
I	up (u), down (d)	e^-, ν_e
II	charm (c), strange (s)	μ^-, ν_μ
III	top (t), bottom (b)	τ^-, ν_τ

anti-particles) have an electric charge and can interact electromagnetically. Neutrinos only interact weakly, and are therefore extremely difficult to detect.

In addition to the fermions which make up matter, the Standard Model also contains another category of particles, the gauge bosons (particles with integer spin), which are the force carriers through which the interactions are mediated. There is a single gauge boson mediating the electromagnetic force (the photon, γ) and three mediating the weak force (Z^0, W^+, W^-), while there are eight kinds of coloured gluons mediating the strong force.

There is one final particle in the Standard Model, the Higgs boson. It is discussed in the next section and it is the only particle predicted by the Standard Model not yet discovered.

2.2 The Higgs Mechanism

The gauge boson fields in a local gauge theory are massless: the presence of a mass term would lead to a non-gauge-invariant Lagrangian. For the weak interaction this is contradicted by experimental evidence – the gauge bosons of the weak interaction are quite heavy, meaning that the symmetry in weak interactions must somehow be broken.

Explicitly breaking the symmetry by directly introducing mass terms in the Lagrangian leads to other theoretical difficulties – the theory becomes non-renormalisable. Instead, one keeps the Lagrangian symmetric, but introduces a symmetry-breaking vacuum. This so-called *spontaneous symmetry breaking* can most easily be accomplished through the *Higgs Mechanism* [2, 3].

Let us introduce an $SU(2)$ doublet with hypercharge $Y = 1$

$$\Phi(x) = \begin{pmatrix} \phi^+ \\ \phi^0 \end{pmatrix}, \tag{2.1}$$

transforming according to

$$\Phi(x) \longrightarrow \Phi'(x) = \exp\left(-\frac{i\tau_j \theta^j(x)}{2}\right)\Phi(x) \tag{2.2}$$

with $\tau_{1,2,3}$ being the Pauli matrices and $\theta^{1,2,3}$ being real functions. Φ couples to the vector fields A^i_μ, B_μ through the following Lagrangian:

$$\mathscr{L}_\Phi = (D_\mu \Phi)^\dagger (D_\mu \Phi) - V(\Phi) \tag{2.3}$$

where the covariant derivative $D_\mu = \partial_\mu - ig\frac{\tau_i A^i_\mu}{2} - i\frac{g'}{2}YB_\mu$. The potential is:

$$V(\Phi) = \mu^2(\Phi^\dagger\Phi) + \lambda(\Phi^\dagger\Phi)^2. \tag{2.4}$$

This potential has, for $\lambda > 0$ and $\mu^2 < 0$, the shape of a mexican hat, with the top of the hat at the origin. It has a minimum for $\Phi^\dagger\Phi = -\frac{\mu^2}{2\lambda}$.

The vacuum expectation value (vev) of a field is the value of the field at the minimum of the potential V. Here, the field gets a non-zero vev

$$\langle\Phi^\dagger\Phi\rangle_0 = \frac{\upsilon^2}{2}, \qquad \upsilon = \sqrt{-\frac{\mu^2}{\lambda}}. \tag{2.5}$$

The symmetry breaking occurs by choosing a certain direction for the vev. The upper component of the Higgs doublet is charged, while the lower is electrically neutral. As the vacuum should be neutral, only the lower component is given a non-vanishing vev while the expectation value of the upper one is set to zero. One obtains

$$\langle\Phi\rangle_0 = \frac{1}{\sqrt{2}}\begin{pmatrix} 0 \\ \upsilon \end{pmatrix}. \tag{2.6}$$

The Higgs field can now be expanded around the vacuum state

$$\Phi = \frac{1}{\sqrt{2}}\begin{pmatrix} \eta_2(x) + i\eta_1(x) \\ \upsilon + h(x) - i\eta_3(x) \end{pmatrix} \tag{2.7}$$

and then inserted into the kinetic part of (2.3). This causes mass terms for the gauge bosons to appear in the Lagrangian, along with interaction terms. By introducing the spontaneous symmetry breaking we have thus given mass to the gauge bosons, as demanded by experimental evidence. However, a problem still remains: massless vector fields have two degrees of freedom (two transverse polarisation directions), while massive fields also have a longitudinal polarisation direction. By making this expansion, we seem to have introduced an inconsistency in the number of degrees of freedom. Fortunately, it can be shown that it is possible to find a suitable gauge transformation (called the unitary gauge) which causes all the massless η fields in our expansion of the Higgs field to be transformed away, being effectively absorbed into the three gauge vector fields (W^+, W^- and Z^0), making up for their longitudinal polarization component. In this way the total number of degrees of freedom is in fact constant. Following this transformation we remain with one massive scalar field unaccounted for – this corresponds to *the Higgs boson*.

The Higgs mechanism also provides mass to all the fermions of the Standard Model, if Yukawa couplings between the fermions and the Higgs field are introduced. The mass of a fermion is then proportional to the strength of the Yukawa coupling between its field and the Higgs field, $m_f = \lambda_f \upsilon/\sqrt{2}$, with λ_f the Yukawa coupling constant.

As mentioned earlier, the Higgs boson is the only particle predicted by the Standard Model that has not been discovered experimentally. For masses be-

low 114.4 GeV, however, it has been excluded at the Large Electron Positron collider (LEP) [9].

2.3 Supersymmetry

2.3.1 Limitations of the Standard Model

The Standard Model is in exceptional agreement with experimental evidence, having been used to predict *e.g.* the $W^{\pm}$ and Z^0 masses before their experimental discovery. Despite its numerous successes, however, there are still problems with the Standard Model, which seem to indicate that there is more physics beyond it.

One experimental disagreement is the observation that neutrinos have a mass [10], in contrast to what the Standard Model postulates. While it is possible to introduce a massive neutrino "by hand", that would provide no explanation for their very low mass. Alternatively, a massive but light neutrino can be introduced by stepping outside of the Standard Model, for example through the so-called see-saw mechanism [11], which also introduces a heavy neutrino partner, typically at a scale of $M \approx 10^{14}$ GeV.

A second experimental problem arises from cosmological observations, such as from WMAP [12], which indicate that only about 4% of the universe consists of matter as described by the Standard Model. About 22% is made up of the mysterious so-called *dark matter*, weakly interacting matter not described by the Standard Model, while the remaining 74% consists of the even more mysterious (and even less connected to the Standard Model) *dark energy* which is responsible for the accelerating rate of expansion of the universe.

At the theoretical level there are also a number of issues, where the Standard Model is found not to be satisfactory:

- The quantization of charge, *i.e* why are all electric charges a multiple of $e/3$ ($-e$ being the electron charge)?
- The observed gap between the masses of the quarks and leptons in the different families. Since the mass of a fermion is given by $m_f = \lambda_f \upsilon/\sqrt{2}$, and the vacuum expectation value of the Higgs field is $\upsilon = 246$ GeV, only the top quark has a "natural" mass scale in the sense that the corresponding Yukawa coupling is of order one ($m_t = 175$ GeV). There is no explanation for the wide variation in fermion masses observed, particularly between the families.
- The considerable variation in the mixing angles between mass eigenstates and interaction eigenstates of the various quarks. The Standard Model provides no explanation as to why they are so different.

- The baryon number asymmetry. The Standard Model provides a single source of CP violation, the Cabibbo-Kobayashi-Maskawa phase – which is insufficient to explain the baryon number of the universe.
- The treatment of gravity. The Standard Model does not in any way include the fourth fundamental force of nature, gravity. Indeed, the fact that a cut-off for the Standard Model has to be introduced, at the highest, at the Planck scale, the scale relevant for gravity, leads to further issues for the Standard Model, such as the hierarchy problem for the Higgs mass, discussed in the next bullet.
- Fine-tuning of the Higgs boson mass. Quadratic divergencies appearing in the Higgs boson mass are proportional to the finite cut-off Λ (often taken at the Planck scale) which has to be introduced in the Standard Model. To one loop order, $m_h^2 = m_0^2 + \delta m_h^2$ with

$$\delta m_h^2 = \frac{3\Lambda^2}{8\pi^2 v^2}(4m_t^2 - 2m_W^2 - m_Z^2 - m_h^2). \tag{2.8}$$

  This means that the bare Higgs mass m_0 (the mass of the scalar field in the absence of quantum corrections) has to be adjusted to more than 30 orders of magnitude[1] in order to cancel them out. This fine-tuning, also called the hierarchy problem, goes against the prejudice that a theory's observable properties should be stable under small variations of fundamental parameters (naturalness).

2.3.2 Supersymmetry in general

To deal with these problems, a number of theories have been proposed, dealing with what is usually referred to as *physics beyond the Standard Model*. Examples of such theories include Technicolor [13], Little Higgs models [14] and theories involving extra dimensions [15].

The theory that has received the most attention, however, is undoubtedly *Supersymmetry* [16], which is a symmetry between bosonic and fermionic fields – in principle a symmetry relating radiation and matter. It implies that each fermion has a corresponding bosonic partner and vice versa, so that the number of fermionic states is equal to that of bosonic states. If supersymmetry were an exact symmetry, then all supersymmetric particles would have the same properties as their ordinary partner except for the spin. This would solve the hierarchy problem, since for an unbroken Supersymmetry the quadratic divergencies caused by Standard Model particles to the Higgs mass would exactly cancel out with the corrections from their corresponding supersymmetric partners, which would have the same mass.

Part of the appeal of Supersymmetry is also that it opens the door for a Grand Unified Theory (GUT), that is a theory in which the electromagnetic,

[1] For $\Lambda = M_P \approx 10^{19}$ GeV.

weak and strong forces all unite at a higher energy scale – in other words that the three fundamental interactions described by the Standard Model are in fact the result of the breaking of a single symmery at some higher energy scale. In the Standard Model such a unification is not compatible with the experimental measurement of the coupling constants – however it is possible to achieve in the presence of Supersymmetry.

Finally, another interesting feature of many supersymmetric models is that they can provide a very good candidate for the dark matter in the universe. If baryon and lepton numbers are generalized to sparticles, [2] the introduction of these fields would allow couplings which violate these numbers. In order to prevent this, a new parity, called R-parity, is introduced. It is defined as $P_R = (-1)^{3B+L+2s}$ with B, L being the baryon and lepton numbers respectively and s being the particle spin. As can be seen, R-parity is defined such that SM particles have $+1$, while sparticles have -1. If this is conserved, then supersymmetric particles can only be produced in pairs, and additionally, the lightest supersymmetric particle (LSP) has to be stable as it can neither decay to ordinary nor to supersymmetric particles. If this LSP does not interact strongly and is electrically neutral, it could very well be what makes up the dark matter.

The picture is somewhat marred, however, by the fact that should Supersymmetry be an exact symmetry, and the sparticles have the same mass as their Standard Model partners, then they should already have been experimentally detected – and they have not. Supersymmetry (if it exists) is therefore said to be broken. This symmetry breaking however has to be done in a careful way (one speaks of "soft" symmery breaking), so as to preserve the desirable features of Supersymmetry, for which it was introduced in the first place. Various models exist for describing this Supersymmetry breaking. They typically consist of having a so-called hidden sector where Supersymmetry is broken. This breaking is then mediated to the visible sector at some higher energy scale, leading to a softly broken Supersymmetry at the electroweak scale. For further details on these models, their phenomenology and on Supersymmetry in general, the interested reader is directed to e.g. [17] and the references therein.

An encouraging characteristic is that in order for the cancellation of the quadratic divergencies to work out, one also needs the mass difference between the Standard Model particles and their superpartners not to be too large. Depending on the specific supersymmetric model and parameters, the lightest superpartners can typically not be much heavier than 1 TeV – an energy range within the reach of the Large Hadron Collider (LHC) at CERN. It is therefore expected that, should it exist, signs of Supersymmetry could be found within

[2] Supersymmetric naming conventions: The supersymmetric partners of the bosons are named by adding the suffix "-ino" to the corresponding field's name, yielding, for example, the gluinos, gauginos and higgsinos. The supersymmetric partners of fermions get their names by adding a prefix "s-" to the corresponding fermion's name (giving, for example, "sbottom", "stop", "squark" etc).

the next years, possibly heralding a new era of exciting particle physics beyond the Standard Model.

2.3.3 The Minimal Supersymmetric Extension of the Standard Model (MSSM)

The MSSM (Minimal Supersymmetric Extension of the Standard Model) is the supersymmetric version of the Standard Model with the minimum number of fields and couplings. It introduces new supersymmetric partners to all of the Standard Model particles. For the SM fermions, each helicity state has its own superpartner, such that for every fermion there exist two superpartners, yielding the selectrons ($\tilde{e}^{\pm}_{L,R}$), smuons ($\tilde{\mu}^{\pm}_{L,R}$), staus ($\tilde{\tau}^{\pm}_{L,R}$), sneutrinos ($\tilde{\nu}$) and squarks ($\tilde{q}_{L,R}$). On the other hand, the superpartners of the SM bosons mix, yielding two charginos ($\tilde{\chi}^{\pm}_{1,2}$) and four neutralinos ($\tilde{\chi}^{0}_{1,2,3,4}$), as well as gluinos ($\tilde{g}$). The MSSM also requires *two* Higgs doublets (as opposed to one in the SM), with hypercharge $Y = \pm 1$. There are two reasons for this. First, the mathematics of Supersymmetry do not allow mixing of left-handed chiral superfields with their conjugates. These however occur in the Lagrangian for fermions – and therefore two Higgs doublets are needed in order to provide mass to both down- and up-type fields, one with $Y = 1$ and one with $Y = -1$. Second, the sum of the hypercharge of all fermions in the Standard Model is zero, thereby exactly cancelling the Adler-Bell-Jackiw, or triangle, anomaly [18, 19]. If there was only one Higgs doublet in the MSSM, there would be only one higgsino with $Y = 1$ and thus the sum of the hypercharges would not be zero, whereas two Higgs doublets imply the existence of a second higgsino with $Y = -1$ which would cancel out the first one. The Higgs sector of the MSSM is the so-called Type-II Two Higgs Doublet Model (2HDM), discussed in more detail in Section 2.4.

In order to accomodate the above particle spectrum, a full 105 parameters need to be added to the existing 19 parameters of the Standard Model (21 masses, 36 real mixing angles and 40 CP-violating phases in the squark and slepton sector, 5 real parameters and 3 CP-violating phases in the gaugino-Higgsino sector). This yields a grand total of 124 parameters in the MSSM, if no assumptions at all are made as to the nature of supersymmetry breaking.

This has led to the emergence of more restricted versions of the MSSM where a number of these parameters are fixed, usually through considerations relating to the mechanism of supersymmetry breaking in a specific model. One of the most popular such models is the *minimal supergravity model* or mSUGRA. Here, the gaugino as well as all scalar masses and the trilinear couplings (which relate to the supersymmetry breaking) are assumed to be equal at the unification scale. With this assumption, only four free parameters and a sign remain, in addition to those of the Standard Model, making it very attractive, in particular when discussing supersymmetry phenomenology at

colliders.

The MSSM is, in a way, the archetype of supersymmetric models, and by far the one that has been studied in most detail – particularly in its mSUGRA version. It must, however, be remembered that the physical motivation for the requirements leading to its minimality are not particularly strong; the reason for its popularity is not so much any evidence that it might be more likely to be realised in nature than other supersymmetric models, but rather convenience. It is minimal and thus easier to handle, and can be thought of as more-or-less representative of a large number of (but by no means all!) supersymmetric models, while at the same time it provides a useful common base for comparisons (for example, of the expected reach of experiments). Thus, many of the results in this thesis dealing with expected experimental reach are presented in the context of the MSSM – but that does not in itself mean that the results are limited to the MSSM.

2.4 Higgs Bosons in the MSSM

The Higgs sector of the MSSM is described by the Type-II Two Higgs Doublet Model (2HDM). However, it should be noted that the 2HDM does not itself require the MSSM – in fact a Type-II 2HDM could be realized in nature even if Supersymmetry is not.

The two Higgs doublets in a Type-II 2HDM (and thus also in the MSSM) must have non-zero vacuum expectation values, since each of them couples to the up- and the down-type fields respectively, and both of these need to be given mass:

$$\langle \Phi_1 \rangle_0 = \begin{pmatrix} v_1 \\ 0 \end{pmatrix}, \qquad \langle \Phi_2 \rangle_0 = \begin{pmatrix} 0 \\ v_2 \end{pmatrix} \tag{2.9}$$

where $Y(\Phi_1) = -1, \quad Y(\Phi_2) = +1$, and $(v_1^2 + v_2^2) = \frac{1}{2}v^2$ with v being the vev in the Standard Model, calculated from the Fermi coupling constant to be 246 GeV. By convention, the ratio of the two vevs is parametrized as:

$$\tan\beta = \frac{v_2}{v_1}. \tag{2.10}$$

Normally v_1 and v_2 are chosen to be positive so that $\tan\beta > 0$.

As was sketched in Section 2.2, three of the four degrees of freedom of the scalar Higgs doublet in the Standard Model are absorbed into the longitudinal components of the three massive vector fields in the unitary gauge, leaving a single massive scalar field. Thus in the SM there exists a single physical Higgs boson. On the other hand, in the 2HDM, having two Higgs doublets gives rise to eight degrees of freedom, of which three are absorbed by the massive

vector fields. Thus five massive scalar fields remain – *i.e.* five physical Higgs particles. For the CP-conserving case, considered in the following, these are:

- two neutral CP-even scalars (typically denoted h^0 and H^0, where $m_h < m_H$),
- one CP-odd scalar (A^0),
- two charged scalars ($H^\pm$).

At tree-level in the MSSM only two parameters are needed to describe the properties of these five particles: $\tan\beta$ and the mass of one of them (very often the mass of A^0 is used, but in a $H^\pm$-specific context it is more natural to use $m_{H^\pm}$). Expressed in terms of $\tan\beta$, m_A and the vector boson masses (m_Z, m_W), the masses of the MSSM Higgs bosons are (always at tree-level) given by:

$$m_{H^\pm}^2 = m_A^2 + m_W^2 \tag{2.11}$$

and

$$m_{H,h}^2 = \frac{1}{2}\left[m_A^2 + m_Z^2 \pm \sqrt{(m_A^2 + m_Z^2)^2 - 4m_A^2 m_Z^2 \cos^2 2\beta}\right]. \tag{2.12}$$

A comprehensive discussion of the Higgs bosons is given in Ref. [20].

2.4.1 Production and decay of charged and heavy neutral Higgs bosons

In the present work, most of the focus lies on charged Higgs bosons at the Large Hadron Collider (LHC). However, Paper IV deals with both charged and heavy neutral (A^0, H^0) Higgs bosons at the proposed Compact Linear Collider (CLIC). Therefore the production mechanism and decay modes for all of these Higgs bosons will be briefly discussed in the following.

2.4.1.1 Production

Production of charged Higgs bosons at the LHC

The production mode of charged Higgs bosons at the LHC depends on its mass: if it is lighter than the top quark, it will predominantly be produced in $t\bar{t}$ events, *i.e* through the process $q\bar{q}, gg \to t\bar{t} \to \bar{t}bH^+$; if it is heavier than the top quark, the main production mechanism will be through gluon-gluon and gluon-bottom fusion, $gg \to \bar{t}bH^+$ (often called the $2 \to 3$ process) and $g\bar{b} \to \bar{t}H^+$ ($2 \to 2$). The $2 \to 3$ and $2 \to 2$ processes are both in fact describing the same underlying process, but under different approximations. Therefore a matching technique needs to be employed, whereby double-counting terms are subtracted, in order to obtain the correct cross-section [21]. The production cross-section depends on $\tan\beta$ and the mass of the charged Higgs boson. Figure 2.1 shows the production cross-section as a function of the charged Higgs boson mass for $\tan\beta = 30$.

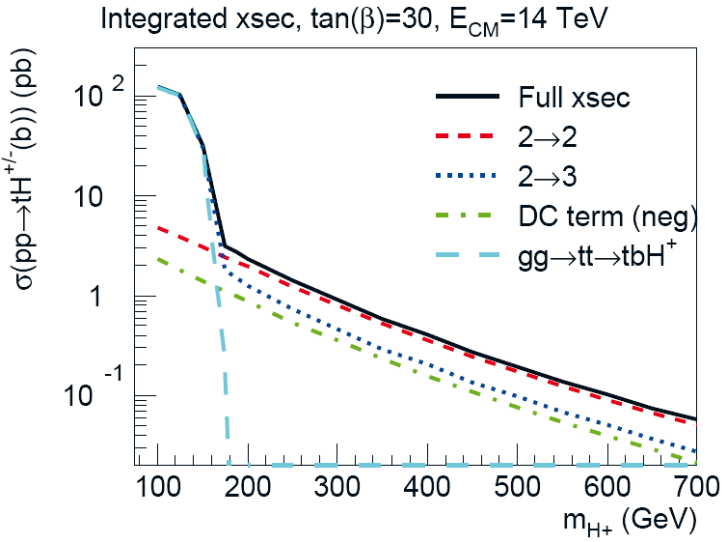

Figure 2.1: Production cross-section for charged Higgs bosons at the LHC with a centre-of-mass energy of 14 TeV and with $\tan\beta = 30$. Also shown is the negative double-counting term which is subtracted from the sum of the other contributions [21].

Other production mechanisms, not considered for the work in this thesis, include production associated with a $W^{\pm}$ boson or with other Higgs bosons.

Production of charged and heavy neutral Higgs bosons at CLIC

In the e^+e^- collisions at CLIC, both the charged and the neutral Higgs bosons will dominantly be produced in pairs via an intermediate Z^0 boson. For the H^0 and A^0 bosons, it is in the following assumed that they are much heavier than h^0 and that $m_A \gg m_Z$. Under these assumptions, $m_A \approx m_H$. The production cross-sections at tree-level only depend on m_A and the centre-of-mass energy $\sqrt{s}$, while they are independent of $\tan\beta$. While the nominal value of $\sqrt{s}$ at CLIC is 3 TeV, the presence of high-energy beam-beam effects (the most important of which is the emission of beamstrahlung photons) leads to a reduction of the actual beam energy at the collision (on average a 16% loss is induced). The resulting spread in the $\sqrt{s}$ distribution, obviously also affects the production of Higgs bosons – this is illustrated in Figure 2.2, showing the production cross-section for $H^{\pm}$ and A^0, H^0 bosons assuming the nominal 3 TeV centre-of-mass energy, and with a more realistic energy distribution including beamstrahlung effects.

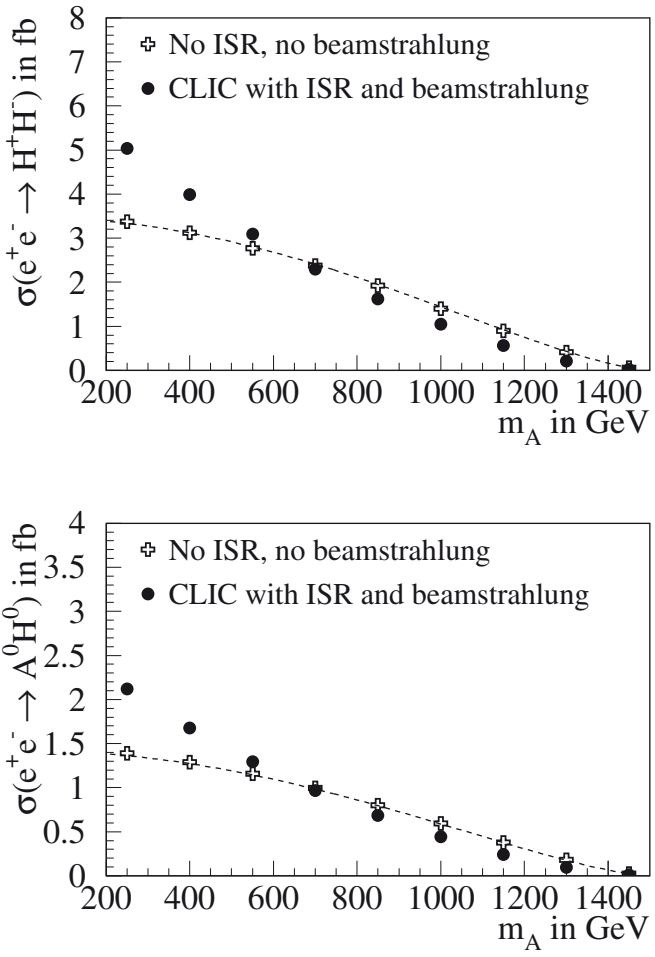

Figure 2.2: Production cross-section for $e^+e^- \to H^+H^-$ (top) and $e^+e^- \to A^0H^0$ (bottom) at CLIC. The crosses show the tree-level cross section as obtained by PYTHIA [22], the dashed line the analytically calculated tree-level cross section, while the full circles show the cross section after taking the beam-beam effects into account. Figure taken from Paper IV.

2.4.1.2 Decays

The focus of this thesis is primarily on the charged Higgs boson decay $H^+ \to \tau^+\nu$ and its charge conjugate, in the following always implied if not explicitly stated. However, the decay $H^+ \to t\bar{b}$ as well as the decays of the heavy neutral Higgs bosons, A^0 and H^0, to $t\bar{t}$, $b\bar{b}$ and $\tau^-\tau^+$ feature in Paper IV so they are all presented in the following. A comprehensive presentation of the decay widths of the Higgs bosons can be found in [23].

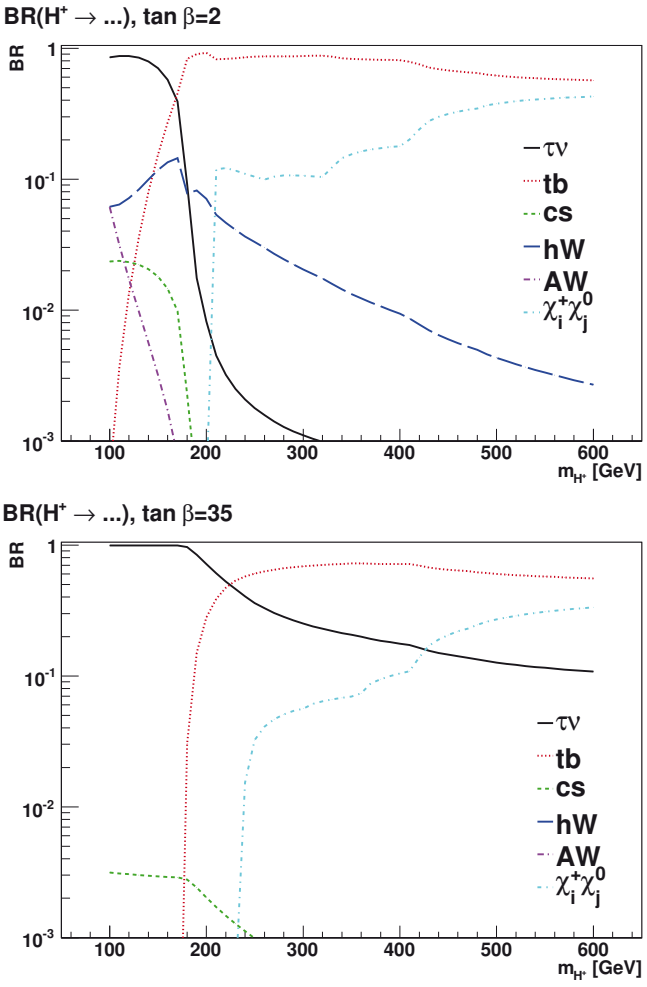

Figure 2.3: Branching ratios for the charged Higgs boson as a function of its mass in the m_h-max scenario of the MSSM, for $\tan\beta = 2$ (top) and $\tan\beta = 35$ (bottom). The calculations were done with FeynHiggs [24].

Charged Higgs boson decays

Figure 2.3 shows the branching ratios of $H^{\pm}$ as a function of its mass for two values of $\tan\beta$ in the so-called m_h-max scenario of the MSSM. This scenario, commonly used when discussing the MSSM Higgs sector, corresponds to a specific choice for the parameters of the model and is designed to maximize m_h for a given $\tan\beta$ [25].

The decay $H^+ \to \tau^+\nu$ dominates for $m_{H^{\pm}} < m_t$, both for low and for high $\tan\beta$. As soon as the $H^{\pm}$ mass exceeds the top quark mass and regardless of $\tan\beta$ value, the decay $H^+ \to t\bar{b}$ becomes the dominant one, while the

$H^+ \to \tau^+\nu$ decay only remains important for large $\tan\beta$ values. The decay to supersymmetric particles becomes comparable to the $H^+ \to t\bar{b}$ decay once it is kinematically allowed.

Heavy neutral Higgs boson (A^0, H^0) decays

The couplings, and therefore the partial decay widths, of the heavy neutral Higgs bosons to both leptons and quarks depend on $\tan\beta$. Figure 2.4 shows the branching ratios of A^0 and H^0 to $t\bar{t}$, $b\bar{b}$ and $\tau^-\tau^+$ in the MSSM, for an A^0 mass of 700 GeV and assuming no decays to supersymmetric particles are kinematically allowed. As can be seen, the decay to $t\bar{t}$ dominates for small $\tan\beta$, while for large $\tan\beta$ the $b\bar{b}$ decay is the most important, with the branching ratio to $\tau^-\tau^+$ also becoming larger. This behaviour is typical for Higgs boson masses larger than the $t\bar{t}$ production threshold, which is the range relevant for the study in Paper IV.

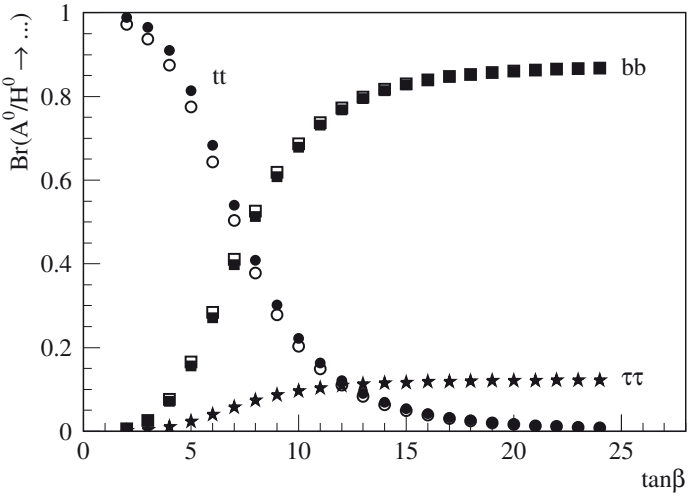

Figure 2.4: Branching ratios for the neutral Higgs bosons in the MSSM (full markers for A^0, open markers for H^0) as a function of $\tan\beta$, for $m_A = 700$ GeV. The behaviour is very similar for other masses above the $t\bar{t}$ threshold, assuming no decays to supersymmetric particles. The branching ratios were calculated using HDECAY [26].

2.4.2 Experimental Constraints

The MSSM Higgs bosons have been searched for both at the Large Electron Positron collider (LEP) at CERN and at the Tevatron at Fermilab.

The lower bounds from LEP are at 92.8 GeV for the lightest CP-even Higgs boson and at 93.4 GeV for the CP-odd boson, in the m_h-max scenario [25].

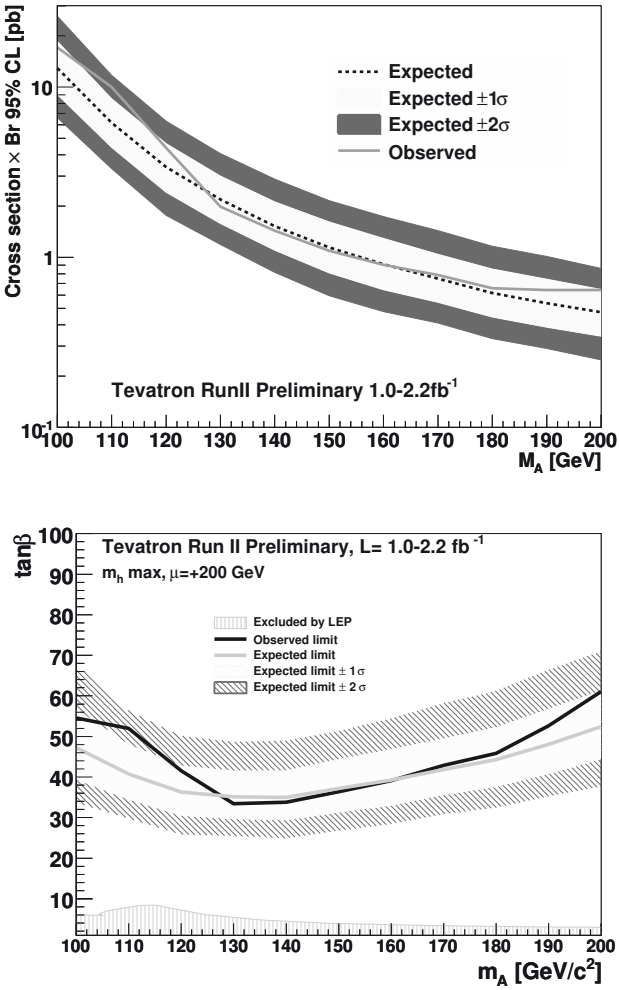

Figure 2.5: Tevatron Run II combined results for MSSM Higgs bosons searches, using the $\phi \to \tau\tau$ channel [27]. Top: excluded cross-section times branching-ratio. Bottom: the same limits translated into excluded contours in the $(\tan\beta, m_{H+})$ plane of the m_h-max scenario.

The LEP results also exclude the $\tan\beta$ regions of $0.7 < \tan\beta < 2.0$, in the same scenario. These bounds, as well as all other exclusions mentioned in this section are at 95% confidence level. As can be seen in Figure 2.5, Tevatron results [27] are also covering certain regions of the $(\tan\beta, m_A)$ parameter space, giving lower limits on $\tan\beta$ which reach almost as low as 30 for masses around 130 GeV, in the m_h-max scenario. For the very heavy mass ranges considered in Paper IV, however, most of the parameter space except for extreme

$\tan\beta$ values is still uncovered. In any case it has to be noted that these limits are very much model-dependent.

For the charged Higgs boson, the LEP lower mass limit lies at 79.3 GeV [28]. Additionally, searches at the Tevatron [29, 30] have for very low and very large values of $\tan\beta$ ruled out a charged Higgs boson with a mass lower than approximately 150 GeV. Complementary to the direct exclusion limits are also the limits that can be obtained indirectly, for instance by looking at meson decays which could be mediated by a charged Higgs should it exist [31]. Examples of such processes include $B \to \tau\nu$, $B \to X_s\gamma$, $B \to \mu^+\mu^-$, $K \to \mu\nu$ and others. Typically such limits (shown e.g. in Figure 2.6) are highly model-dependent.

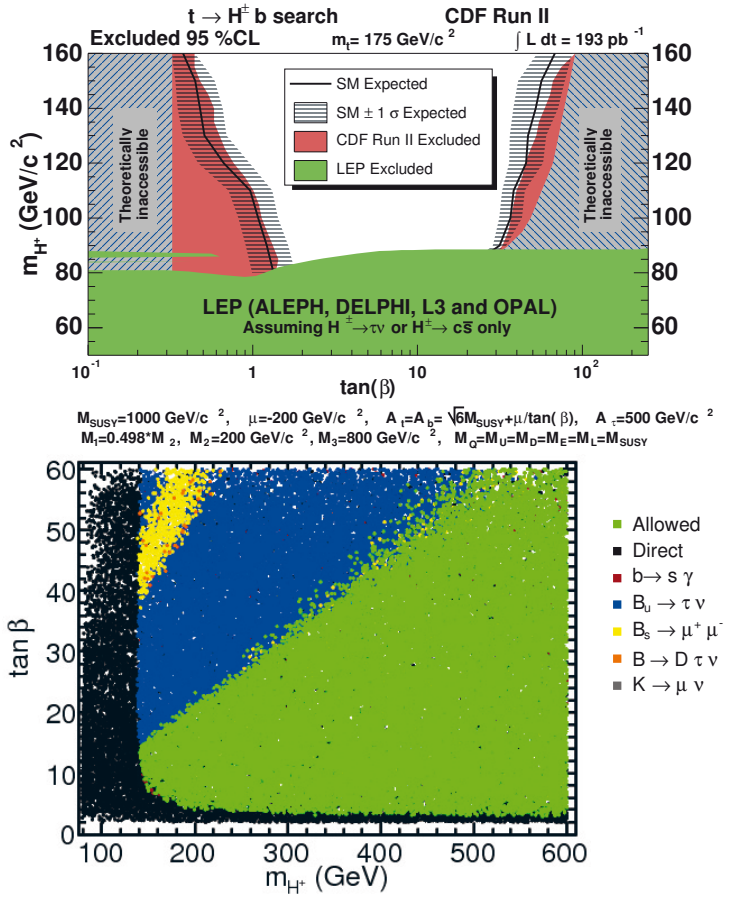

Figure 2.6: Top: Excluded regions in the $(\tan\beta, m_{H+})$ parameter space in the m_h-max scenario, from LEP and the CDF experiment at the Tevatron [29]. Bottom: Indirect exclusion limits for the charged Higgs boson in Non-Universal Higgs Mass scenaria [31].

3. Accelerators and Detectors

3.1 The Large Hadron Collider

The Large Hadron Collider (LHC) [1] is the world's largest and most powerful man-made particle accelerator. It is built and maintained by the European Organization for Nuclear Research (CERN), close to the French border outside of Geneva, Switzerland. The LHC is installed 50-175 m underground and is circular, with a circumference of 27 km. It is designed to collide protons as well as lead ions at four interaction points around the ring.

The LHC had its first collisions on the 23rd of November 2009 at the injection energy (450 GeV per beam), with higher energy collisions following shortly thereafter. A final centre-of-mass energy of up to 14 TeV is envisaged when operating in the $p-p$ mode, for which the design parameters are given in Table 3.1.

Table 3.1: *Design parameters of the LHC, for injection and for 14 TeV collisions [32].*

Parameter	Unit	Injection	Collision
Beam Data			
Proton Energy	[GeV]	450	7000
Proton revolution frequency	[Hz]	11245	
Number of particles per bunch		1.15×10^{11}	
Number of bunches		2808	
Circulating beam current	[A]	0.58	
Stored energy per beam	[MJ]	23	362
Beam current/Luminosity lifetime	[h]	-	18 / 15
Bunch spacing	[ns]	25	
Events per bunch-crossing		-	19.02
Ring Parameters			
Ring circumference	[m]	26659	
Number of magnets		9593	
Number of main (dipole) bends		1232	

At each of the four interaction points stands the detector of one of four large-scale experiments utilizing the LHC: CMS [33] and ATLAS [4] are general-purpose experiments which will be searching for a wide range of possible new

physics processes and particles, such as the Higgs boson or Supersymmetry. These detectors have almost full spherical coverage of the interaction point, and will provide precise measurement and identification of electrons, muons, jets and more. LHCb [34] and ALICE [35] on the other hand are focusing on more specific areas and their detectors are thus much more specialized: LHCb is dedicated to the precision measurements of CP violation and of rare decays, in particular of hadrons containing bottom quarks. ALICE is specialised towards the heavy ion collisions and intends to study the behaviour of nuclear matter at high densities and energies, where the formation of quark-gluon plasma, a new phase of matter, is expected.

3.2 The ATLAS Experiment

The cylindrical ATLAS detector, shown in Figure 3.1, is the largest of the four LHC detectors, measuring about 25 m in diameter and approximately 46 m in length and with a total weight of roughly 7000 tons. Being a general-purpose experiment, ATLAS has been designed to be sensitive to as wide a range of physics as possible, exploiting the full LHC potential. Phenomena and particles which might be found or excluded with the ATLAS detector include Supersymmetry, Higgs bosons, mini black holes, and more. To this end, ATLAS consists of several layers of sub-detectors, each designed for specific purposes in terms of particle tracking, energy measurement etc. A full and detailed description of the various components of the ATLAS detector can be found in Reference [4], on which the following briefer descriptions are based.

3.2.1 The Inner Detector

The ATLAS Inner Detector (Figure 3.2) is designed to provide high precision tracking in both the $R-\phi$ and z coordinates. It consists of three sub-systems, the Pixel detector, the Semi-Conductor Tracker (SCT) and the Transition Radiation Tracker (TRT), and it is immersed in a 2T magnetic field generated by the ATLAS central solenoid, extending over a length of 5.3 m at a diameter of 2.5 m, centred at the nominal interaction point. The Pixel detector and SCT cover a region in pseudorapidity[1] of $|\eta| < 2.5$ while the TRT reaches up to $|\eta| = 2.0$.

The Pixel detector provides the highest granularity and is located closest to the vertex region. There are three pixel layers, segmented in $R-\phi$ and z, arranged in concentric cylinders around the beam axis in the barrel region, while in the end-cap regions they are arranged on disks perpendicular to the

[1]The pseudorapidity is defined as $\eta = -\ln\tan(\theta/2)$, with the polar angle θ being the angle from the beam axis.

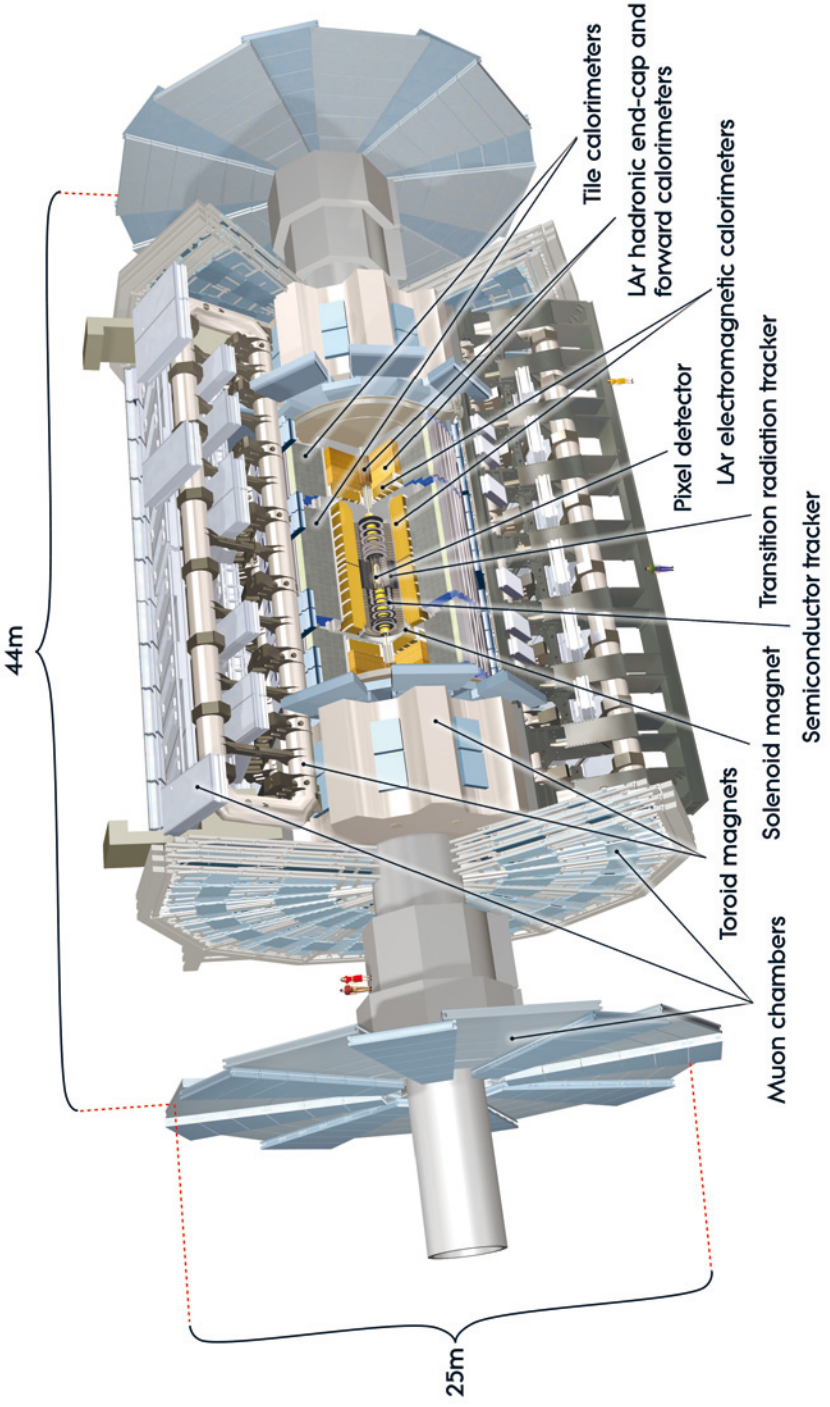

Figure 3.1: Cut-away view of the ATLAS detector with the principal components marked.

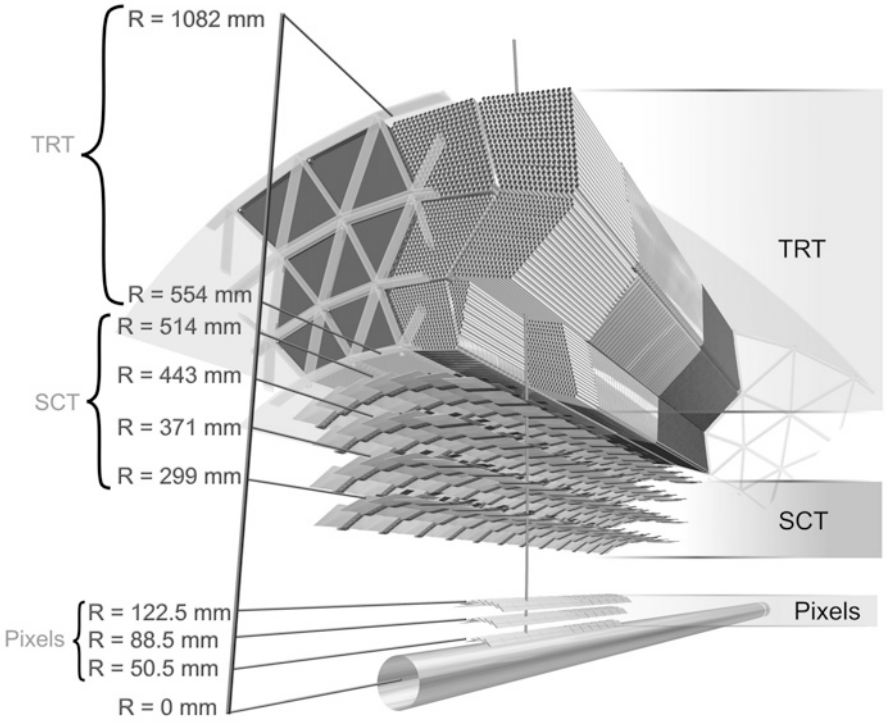

Figure 3.2: Cross-section of the ATLAS Inner Detector barrel.

beam axis. The intrinsic accuracies are 10 μm ($R-\phi$) and 115 μm (z) in the barrel, and 10 μm ($R-\phi$) and 115 μm (R) in the endcaps.

The SCT consists of four double-sided layers in the barrel region and nine disks in each of the endcaps. It is described in more detail in Section 3.3.

The TRT consists of 4 mm diameter straw tubes filled with Xenon gas. In the barrel region the straws measure 144 cm in length, running parallel to the beam axis, with their wires divided at approximately $z = 0$. In the endcaps the 37 cm long straws are radially arranged on wheels. The TRT provides only $R-\phi$ information with an intrinsic accuracy of 130 μm per straw but with an average of 36 hits per track – the lower precision per point being compensated by the larger number of measurements and the longer measured track length. Additionally, the TRT provides for enhanced electron identification through the detection of transition radiation photons in the gas of the straw tubes.

3.2.2 The Calorimeters

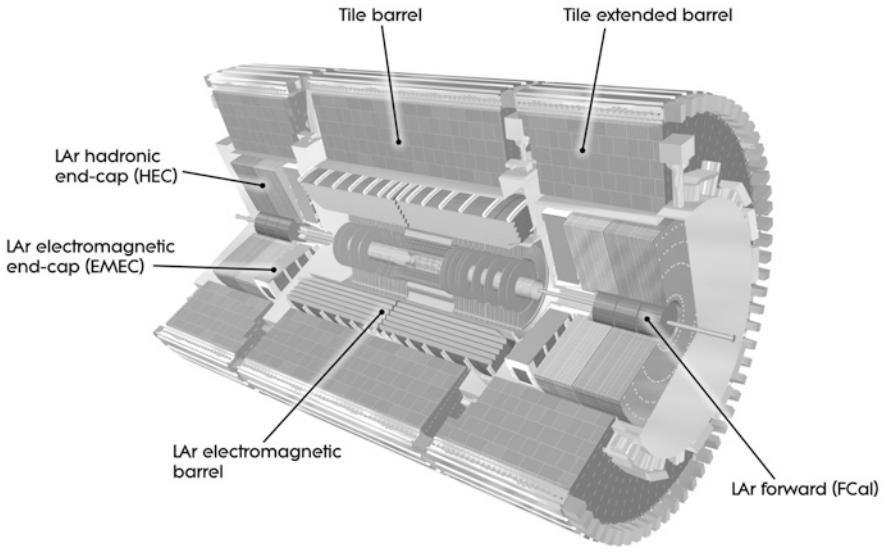

Figure 3.3: Cut-away view of the ATLAS calorimeters.

The electromagnetic and hadronic calorimeters of ATLAS (Figure 3.3) cover the range of $|\eta| < 4.9$, with the η region matched to the inner detector having a finer granularity in the EM calorimeter, as suited for precision measurements of e.g. electrons and photons.

The electromagnetic calorimeter consists of accordion-shaped kapton electrodes and lead absorber plates. It is filled with liquid Argon (LAr), which is the detecting material. It is divided into the barrel ($|\eta| < 1.475$) and the two end-caps ($1.375 < |\eta| < 3.2$). The barrel is further divided into two identical halves, with a 4 mm gap at $z = 0$. The two end-caps are each in turn divided in two coaxial wheels, separated at $|\eta| = 2.5$, with the inner wheel having a coarser lateral granularity and two sections in depth as opposed to three for the rest of the calorimeter. A presampler, consisting of a 1.1 cm (0.5 cm in the end-cap) active LAr layer, is present in the region of $|\eta| < 1.8$, used to correct for the energy that electrons and photons loose upstream of the calorimeter.

Three types of hadronic calorimeters are used, depending on the covered η region. The Tile Calorimeter covers the region up to $|\eta| = 1.7$. It uses steel as the absorber and scintillating tiles as the active material, with two sides of the tiles read out by wavelength shifting fibres into two separate photomultiplier tubes. The region going from the Tile Calorimeter up to $|\eta| = 3.2$ is covered by the Hadronic End-cap Calorimeter (HEC) which consists of two

independent wheels per end-cap directly behind the end-cap EM calorimeter. The HEC uses copper as the absorber and LAr as the active material. Finally, the Forward Calorimeter (FCal) covers the most forward region up to about $|\eta| < 4.9$. It consists of three modules in each end-cap, the first made of copper and the other two of tungsten, with LAr as the active material.

3.2.3 The Muon System

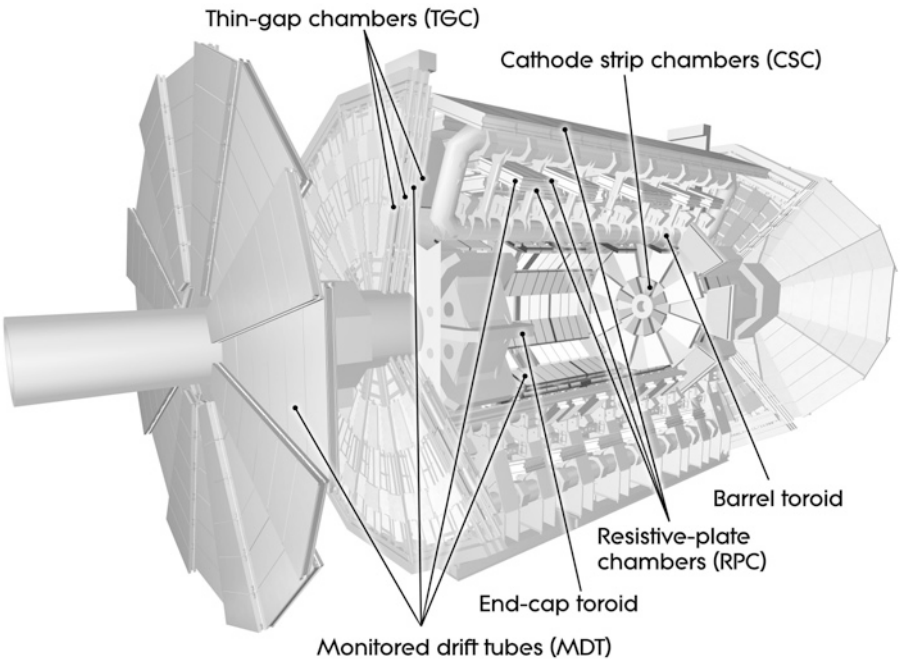

Figure 3.4: Cut-away view of the ATLAS muon system.

The ATLAS muon spectrometer (Figure 3.4) is based on the deflection of muon tracks as they pass through the magnetic field of the large superconducting air-core toroid magnets. In the central barrel part of the muon spectrometer the magnetic field is provided by the large barrel toroid for ranges up to $|\eta| = 1.4$. In the end-caps, $1.6 < |\eta| < 2.7$, two smaller magnets provide the magnetic field, while for the transition region $1.4 < |\eta| < 1.6$ it is provided by a combination of the barrel and end-cap fields.

Three layers of Monitored Drift Tubes (MDTs) are used over most of the η-range for the precision measurement of muon tracks in the bending direction of the magnetic field. For pseudorapidities of $2 < |\eta| < 2.7$, multiwire proportional chambers called Cathod Strip Chambers (CSCs) are used in the innermost plane, due to the demanding particle rate.

To obtain the muon coordinate in the direction orthogonal to the precision-tracking chambers, as well as for triggering, Resistive Plate Chambers (RPCs) are used in the barrel and Thin Gap Chambers (TGCs) in the end-caps.

3.2.4 The Trigger

Due to the high instantaneous luminosity expected at the LHC (up to 10^{34} cm^{-2}s^{-1}), a very efficient triggering system is required: at the design luminosity the expected interaction rate is around 1 GHz while the data recording is limited to approximately 200 Hz. Thus an excellent rejection against minimum bias processes is required, while at the same time maximum efficiency for new physics processes is required. The ATLAS trigger is divided into three levels (L1, L2 and Event Filter), with the last two collectively referred to as the High-Level Trigger.

The L1 trigger system only uses limited detector information from the muon spectrometer and calorimeters, to make a decision in less than 2.5 μs, reducing the rate to approximately 75 kHz. The trigger decision is based on the missing transverse energy, the total transverse energy or the transverse momentum of electrons, photons, muons, jets or hadronically decaying tau-leptons. The L1 trigger defines one or more Regions-of-Interest (RoIs) in the η and ϕ coordinates of a selected object. If an identified object passes specified criteria, the event is forwarded to the next trigger level along with its corresponding RoIs – if not, the event is discarded and lost for ever.

The L2 trigger system, seeded by the L1, uses all of the available detector data within the relevant RoIs. The trigger decision is done within about 40 ms, reducing the data rate to about 3.5 kHz. Surviving events are then passed on to the Event Filter which uses almost offline-equivalent analysis procedures to make a final decision on the event, within a time of the order of four seconds. After the Event Filter the rate is reduced to approximately 200 Hz. Events reaching this stage are moved on to the CERN computer centre to be processed offline for permanent storage.

3.3 The ATLAS Semi-Conductor Tracker (SCT)

The ATLAS Semi-Conductor Tracker (SCT) resides between the Pixel detector and the TRT in the Inner Detector. It consists of four double-sided layers in the barrel region and nine end-cap disks at each end, outfitted with silicon micro-strip detector modules for high precision spatial measurement of charged tracks. The intrinsic accuracies of a layer in the barrel is 17 μm in $R-\phi$ and 580 μm in z, while in the end-cap it is 17 μm ($R-\phi$) and 580 μm (R) in the end-cap.

The SCT barrel modules are built of micro-strip silicon sensors segmented into 768 strips of 80 μm pitch, measuring $63.96 \times 63.56 \times 0.285$ mm^3. The

modules are double sided, and each side has two strip sensors, wire-bonded to each other for a total strip length of 126 mm per side and connected to binary signal readout chips. The two sides of a module are rotated with a stereo angle of 40 mrad to enable measurement of the third coordinate of the space-point formed by correlating hits on both sides of the module. Between the two sides a 380 μm-thick thermal pyrolitic graphite (TPG) base-board is glued, providing the module with both mechanical and thermal structure, but also with the electrical path for the high voltage to the sensor backplane. The end-cap modules come in three different types, depending on their position on the end-cap disks but like the modules in the barrel they all have two sets of sensors glued back-to-back at a stereo angle of 40 mrad.

3.3.1 Commissioning of the SCT with Cosmic Rays

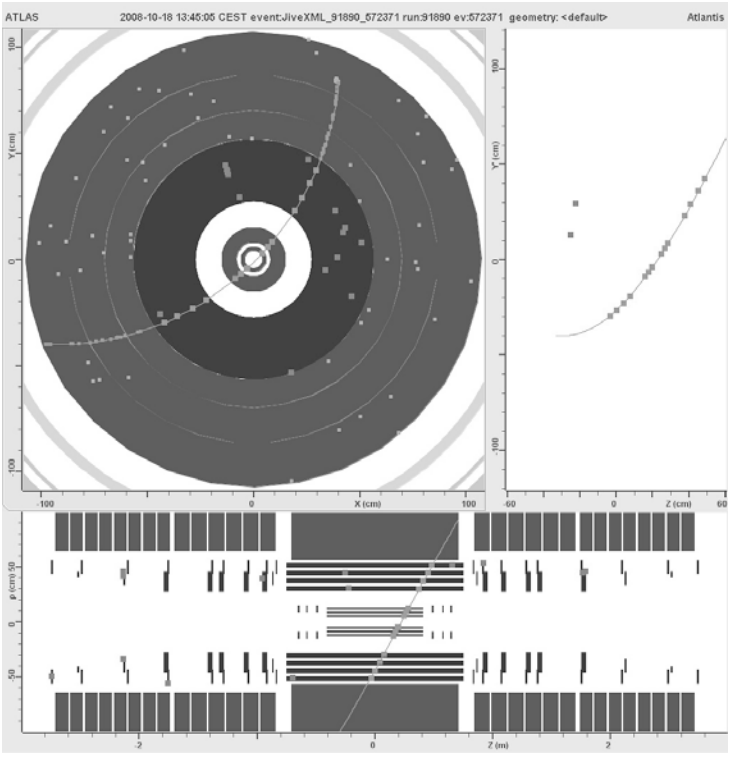

Figure 3.5: A typical event passing through the ATLAS Inner Detector barrel, recorded in the 2008 cosmic-ray run [36].

An important step in the commissioning of the ATLAS detector in general, and of the SCT in particular, has been the collection of cosmic-ray data. During 2008 and 2009 several campaigns of data collection were performed for

the whole ATLAS detector, as well as individually for the SCT, both with and without the solenoid magnetic field. Such campaigns constitute an excellent test of the detector itself, its integration with the rest of ATLAS, as well as of both the online and offline software and the Detector Control System. Furthermore, due to the geometric distribution of cosmic rays, which is substantially different from that of beam collisions, they are particularly suitable for certain studies: The wide angular range of the cosmic rays allows for the extraction of modes in the tracker that cannot be reached with tracks only originating from the interaction point. For other studies, analysis of cosmic ray data allow the measurement and characterization of aspects of the detector before collisions actually take place. Analysis of the cosmic-ray data also constitutes a test of the software infrastructure used to access the recorded data, in preparation for the actual collisions data analysis. In this way both the software is excercised, as well as the physicists meant to use it.

One of the most extended cosmic-ray data-taking campaigns took place in the fall of 2008. A number of SCT studies were developed and performed using that set of data. Examples of such studies include the measurement of the intrinsic SCT efficiency, investigation of dead channels, measurement of the SCT noise occupancy, studies of the depletion depth, and, most relevantly for this thesis, measurement of the SCT Lorentz angle.

The Lorentz angle is the angle in the drift of the charge carriers inside the silicon that arises due to the presence of the solenoidal magnetic field. The Lorentz angle depends on detector operating conditions, such as the bias voltage and the temperature, through the electron and hole mobility. For a 2 T magnetic field the Lorentz angle in the SCT is estimated to be about 4 degrees – corresponding to a 20 μm shift in the silicon sensor, which is comparable to the 80 μm strip pitch. The Lorentz angle is important for detector alignment, cluster size determination and spatial resolution. So far the theoretically predicted value of the SCT Lorentz angle is used for these purposes and an experimental measurement is thus quite important, in order to verify or correct the angle from the model. An additional reason to measure the Lorentz angle before the detector has been exposed to significant radiation is to enable a comparison with measurements taken after substantial irradiation, allowing for studies of the effects of radiation damage. Finally, as the SCT uses a binary readout, the Lorentz angle also serves as an important observable for studying various aspects of the detection process itself, which are not directly accessible in the digital signal – any unexpected behaviour might show up as a deviation from the expected value.

3.4 Determination of ATLAS Physics Potential

In anticipation of the actual proton-proton collisions at the LHC, a great number of studies have been performed in order to determine the physics potential

of the various detectors. Such studies are not only useful in that they give the particle physics community an idea of what to expect, but they are also (and in a sense, primarily) important because in order to be performed, a great number of data-analysis methods and tools have to be developed and tested.

3.4.1 Simulation

Instead of real data, physics potential studies utilize simulated Monte Carlo events. Specialized programs called event generators (such as *e.g.* PYTHIA [22]) are used to simulate interesting processes (such as the production and subsequent decay of a charged Higgs boson) using Monte Carlo techniques. The output of each generated event is a list of all intermediate and final particles, with their momenta, energies and masses, along with information about which particle they were produced from, and what they have subsequently decayed into, so that one can follow in detail how the event developed. This event listing, commonly referred to as the *truth information* of the event, is then fed into a very detailed simulation of the detector response performed using a simulation tool-kit for particle-matter interactions, GEANT4 [37]. This is followed by a simulation of the digitization of the signal from the detector. The output of the digitization is then fed to the same physics-objects reconstruction and identification algorithms prepared for real collisions data. It is on their output that the data analysis algorithms are typically run.

3.4.2 Analysis

For a typical simulation study, one needs to consider not only signal events but also the background – that is to say, events from other processes than the one to be studied which either through similar final states or through detector or reconstruction effects, such as misidentified physics objects, look like the signal. The challenge in an analysis, both simulated and on real data, is to devise a selection such as to suppress the background while retaining the signal. This can be done in a number of ways, such as sequential cuts (requiring that certain quantities in each event fulfill set requirements, *e.g.* at least 3 jets of 15 GeV transverse momentum) or multivariate techniques (such as likelihoods, boosted decision trees, etc). Typically the signal will then consist of an excess over the expected number of background events. It is obvious that a very good understanding of the background processes is needed in order to be able to show that any excess is not just a statistical fluctuation. Additionally one needs to carefully consider systematic effects and their associated uncertainties and how these affect both the signal and the background.

To this end, a complete analysis is not limited to defining the appropriate selection for enhancing the signal over the background, but also includes development of methods for the determination of the systematic uncertainties, of

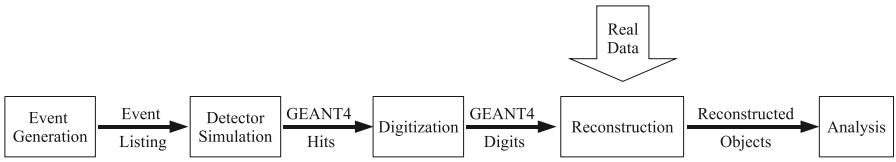

Figure 3.6: Schematic representation of the data flow for simulated events in the ATLAS detector.

the efficiency and fake-rates, of the background shape and normalization, etc. Usually in simulation studies an estimated value for these quantities has been assumed, but with real, high-energy collisions approaching, the development of such methods is becoming a major focus.

With all these effects and more taken into account, the final step in a simulation study is to actually obtain the discovery (exclusion) potential for the given process by determining the possible parameter ranges for which a statistically significant[2] discovery (exclusion) will be possible, as well as the amount of collected data needed, typically expressed in terms of *integrated luminosity*.

Every effort is made to ensure that the simulated samples are as close as possible to what one expects to see once the detector starts collecting real collision data. However, it is a very real possibility that the data may look quite different from what one expects from the simulation – meaning that many methods and tools developed with simulated samples might have to be reoptimised or even redesigned. A lot of effort will also have to go into understanding and quantifying the efficiencies, fake-rates, systematics etc. It is therefore important to understand that the integrated luminosities mentioned in simulation studies in most cases refer to the integrated luminosity with a well-understood detector – thus a discovery claimed to be possible with 100 pb^{-1} does not necessarily refer to the *first* 100 pb^{-1} collected by the detector.

3.5 Beyond the LHC

The LHC will allow the exploration of many regions of physics not reachable until now. Should it exist, a SM-like Higgs boson will most likely be discovered and Supersymmetry, as well as a number of other theories of physics beyond the SM, will be probed over a large region of their parameter space. An upgrade of the LHC is already being planned – the SLHC, or Super Large Hadron Collider, which would feature higher centre-of-mass energy and/or instantaneous luminosity, further expanding the potential for exciting discov-

[2]Typically, to claim a discovery the probability for a potential signal not to be a fluctuation of the background is required to be at least 5σ, while for an exclusion a 95% confidence level is required.

eries. Nevertheless, the physics reach of the (S)LHC, impressive though it is, has of course also its limits in energy and precision. A successor to the LHC will therefore be necessary for further discoveries and precision measurements of particles discovered at the LHC. Such a project would of course be enormous, just as the LHC is, with planning, design and construction requiring a time comparable to the foreseen life-time of the LHC as an accelerator. It is in the nature of the titanic undertakings required by modern particle physics, that designing of the next facility has to begin before the current one has even started operation. The particle physics and accelerator technology communities have therefore already begun thinking about and actively working on the LHC's successor.

It is of course a great challenge to specify requirements for the LHC's successor before knowing anything about the physics results produced at the LHC. The two most prominent proposed concepts are both for a linear e^+e^- collider. The collision of leptons leads to much cleaner events compared to proton-proton collisions, where several partons interact, leading to a complicated underlying event. This is desirable for precision measurements, *e.g.* of new particles and phenomena potentially discovered at the LHC. The choice of a linear collider rather than a circular is due to the enormous energy loss from synchrotron radiation in a circular e^+e^- collider of comparable energy.

The first concept, the International Linear Collider [38] (ILC), proposes the use of superconducting accelerating structures (a known technology) for accelerating the electrons and positrons, colliding them at centre-of-mass energies of 500 GeV. It would be about 31 km in length (plus two damping rings of some 6 km circumference), with an accelerating gradient of 31.5 MV/m. By increasing its length, the ILC can be upgraded to 1 TeV. The second, the Compact Linear Collider [5] (CLIC) proposes a completely novel acceleration technique, foreseen to collide electrons and positrons at centre-of-mass energies of up to 3 TeV. As it forms the context for Paper IV it will be described in more detail in the following section.

No final decision has as yet been made as to which of the two concepts to follow, and most probably results from the LHC will influence such a decision. Until a decision is reached, R&D is ongoing for both concepts – in fact part of it in common for both of them, as many aspects of the design are similar.

3.5.1 CLIC

The CLIC proposal is based on the so-called two-beam acceleration technology, which consists of two beams running in parallel – the main beam and the drive beam. The key concept is that the RF power required by the accelerating structures of the main beam is extracted from the drive beam, which is running at low energy but high intensity (2.37 GeV, 11.9 GHz, 101 A). This allows use of travelling wave structures with accelerating gradients reaching up to

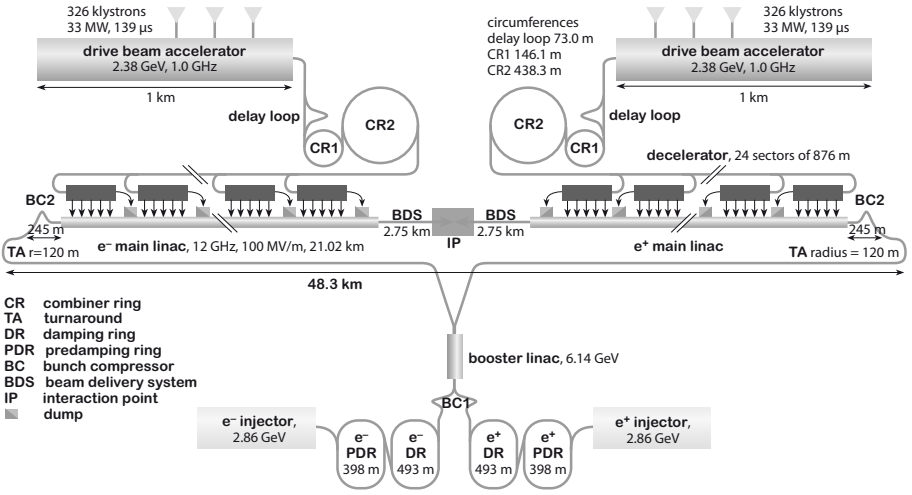

Figure 3.7: General layout of the Compact Linear Collider [39].

120 MV/m.[3] This high gradient significantly reduces the length (and thus the cost) of the linear accelerator. In total 24 drive beams will be required for accelerating the main beams up to 1.5 TeV each.

It should be noted that at CLIC a number of high-energy beam-beam effects come into play just prior to the collision and need to be taken into account, especially when considering the physics potential of the collider. Due to the very small transverse size of the beams at the interaction point, the electrons/positrons in one beam experience very strong transverse electromagnetic forces from the moving charges in the other beam. This causes their trajectory to be bent, inducing the emission of photons (*beamstrahlung*) and thereby loss of energy. An effect of this is illustrated in Figure 3.8, showing the expected centre-of-mass energy spectrum at CLIC, which displays a peak just below the nominal 3 TeV but also a very long tail down to very low energies. In addition, the emitted beamstrahlung photons may collide with each other, producing a hadronic background to the e^+e^- collisions. These effects are not negligible – at a luminosity of 6×10^{34} cm^{-2}s^{-1}, the luminosity that is above 99% of the nominal centre-of-mass energy is about 2×10^{34} cm^{-2}s^{-1}, while the average number of hadronic events produced by beamstrahlung photon collisions are 2.7 per bunch crossing [40].

Tests of the CLIC technology are currently being performed at CTF3 (CLIC Test Facility 3), at CERN, with the purpose of determining the feasibility of the proposed technical solutions by 2010. At the same time, simulation studies

[3]The reader should be aware that these parameters have changed since Paper IV was written. At that time, the design drive beam frequency was 30 GHz and the accelerating gradient 150 MV/m.

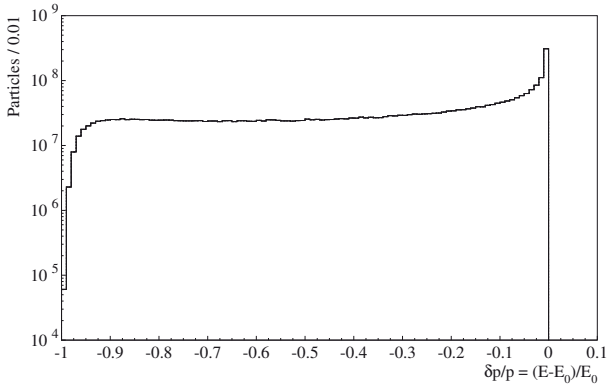

Figure 3.8: Centre-of-mass energy spectrum of CLIC. Figure taken from Ref [41].

of both the discovery potential and the accuracy with which new phenomena can be measured at such a collider are also performed, in order to be able to assess its physics performance and provide feedback in early stages of its design and/or construction.

As no detector design for CLIC existed at the time of writing Paper IV, that study, and other contemporary ones, assumed a very generic detector set-up, based on the detector R&D for the ILC, and simulated the detector response by a parametrized smearing of the various final-state particles' four-vectors.

4. Tau-Jet Reconstruction and Identification in ATLAS

4.1 The Tau Lepton

The tau lepton (τ) was discovered at SLAC (Stanford Linear Accelerator Center, USA) in 1975. Its name is derived from the Greek word for "third", τρίτον, as it is the charged lepton of the third generation. It has a mass of 1776.84 ± 0.17 MeV and a mean life time of $(290.6 \pm 1.0) \times 10^{-15}$ s [42].

The tau lepton decays to a lighter lepton and two neutrinos with a branching ratio of about 35%. The rest of the times it decays hadronically, being the only lepton that is heavy enough for such a decay. The hadronic decays of the τ are dominated by the production of $\pi^{\pm}$s along with a neutrino and possibly one or more π^0s. There are also decay modes involving kaons, but they are substantially rarer. Table 4.1 summarizes the tau decay modes.

In ATLAS the main interest in the tau lepton arises from many interesting physics processes which include a tau lepton in the final state. Being able to efficiently detect tau leptons is important both for measurements of properties of SM particles, such as the $W^{\pm}$ and Z^0 bosons or the top quark, but also for the potential discovery of new particles and phenomena, such as a low-mass SM Higgs boson, neutral MSSM Higgs bosons, supersymmetric particles and, most crucially for this thesis, charged Higgs bosons (whose decay $H^{\pm} \to \tau\nu$ dominates at low masses).

From a detection point of view, distinguishing the leptonic modes from primary leptons would be difficult – therefore, these decays are considered in the same way as the reconstruction of the corresponding lepton. Thus with reconstruction of τ leptons, the reconstruction of the hadronic decay modes is usually meant. One therefore commonly speaks of the reconstruction and identification of *tau-jets*.

4.1.1 The Tau-Jet

When discussing tau-jets one usually distinguishes between the 1-prong and the 3-prong case, where the number of prongs corresponds to the number of charged pions the tau lepton decayed to.

In both cases, the experimental signature is that of a collimated jet. It is required to be isolated from the rest of the event, with low track multiplicity, and relatively narrow depositions in the calorimeters, often with a relatively large

Table 4.1: *Tau decay branching ratios, as given in Ref. [42]. $h^{\pm}$ signifies a $\pi^{\pm}$ or $K^{\pm}$ meson, and n a π^0 meson or a photon.*

Type	Decay mode	Branching ratio
one prong leptonic	$e^- \bar{\nu}_e \nu_\tau$	17.9%
	$\mu^- \bar{\nu}_\mu \nu_\tau$	17.4%
one prong hadronic	$h^- \nu_\tau$	11.6%
	$h^- \nu_\tau \geq 1n$	37.1%
three prong	$h^- h^- h^+ \nu_\tau$	9.8%
	$h^- h^- h^+ \nu_\tau \geq 1n$	5.4%
five prong	$h^- h^- h^- h^+ h^+ \nu_\tau \geq 0n$	0.1%

electromagnetic component due to the π^0s decaying to photons (particularly true for 1-prong decays due to the larger branching ratio for decays involving π^0s).

4.2 Reconstruction and Identification

In ATLAS the reconstruction of tau-jets is performed using two complementary algorithms: one which starts from tracks as seeds for the reconstruction of τ candidates and one using calorimeter cells as the seed. The achieved reconstruction efficiency with a combination of the two algorithms is high, but it also allows for a large number of fake candidates primarily from QCD jets. This calls for a second step, called identification, where a number of discriminating variables are used to discard fake candidates in order to achieve adequate purity [43]. The tau-related work for this thesis has focused exclusively on the identification stage.

4.2.1 Reconstruction

The two reconstruction algorithms differ not only in the seed used, but also in their scope, as the track-seeded one is more exclusive, while the calo-seeded one is broader in scope and relying on the identification stage to remove any fakes. The track-seeded algorithm is run first, and for each track seed, a seed for the calorimeter-seeded algorithm is also searched for within a cone of $\Delta R = 0.2$. If none is found, the tau candidate is considered a track-seed-only candidate. If a seed is found, the calorimeter-based reconstruction is also run, information from the two algorithms merged and the resulting tau candidate is considered reconstructed by both algorithms. Finally the calorimeter-seeded

algorithm is run on all its remaining seeds, and any resulting candidates are considered as calorimeter-seed-only candidates. For $Z^0 \rightarrow \tau\tau$ events, about 70% of the τ candidates are reconstructed by both algorithms, about 25% only by the calorimeter-seeded, and approximately 5% only by the track-seeded.

4.2.1.1 Track-seeded Reconstruction

The track-seeded reconstruction starts by selecting good-quality tracks, fulfilling the following requirements, where the transverse impact parameter (d_0) is the distance of closest approach of the track to the reconstructed primary vertex in the $R-\phi$ projection:

- $p_T > 6.0$ GeV
- $d_0 < 1$ mm
- track fit χ^2/ndf< 1.7
- # Pixel + SCT Hits ≥ 8
- # low threshold TRT hits ≥ 10 (for $|\eta| \leq 1.9$)
- # high threshold TRT hits ≤ 5 (loose veto versus electron tracks).

Thereafter, an isolation requirement is made, demanding that there be at most 2 additional tracks passing these cuts, with the transverse momentum cut reduced to $p_T > 1.0$ GeV, within a cone of $\Delta R \leq 0.2$ around the seed (*core* region), while no tracks are allowed in the isolation region, $0.2 < \Delta R < 0.4$. If no additional tracks are found in the core region, the candidate is treated as a 1-prong tau candidate, otherwise it is treated as a 3-prong candidate. Its energy is then estimated using the energy flow approach, where the calorimeter deposits from charged particles, *i.e.* clusters which are associated with a track, are replaced by the track momenta. The neutral particle contribution is then included, after correcting for the effects of both π^0 and $\pi^{\pm}$ depositing energy in the same calorimeter cells.

4.2.1.2 Calorimeter-seeded Reconstruction

An algorithm for topological clustering is used to identify Topological Clusters in the calorimeter, out of which a *TopoJet* can be constructed by combining clusters within a cone of 0.4 in ΔR. A TopoJet is retained if it has $E_T > 10$ GeV and $|\eta| < 2.5$, at which point tracks are associated to it, if they are within $\Delta R < 0.3$ of the TopoJet centre and pass the following quality selection criteria:

- $p_T > 1.0$ GeV
- $d_0 < 1.5$ mm
- track fit χ^2/ndf< 3.5
- # Pixel + SCT Hits ≥ 6
- # Pixel + B-layer Hits ≥ 1.

The tau candidates are then passed on to the identification stage for the separation of the signal from fakes.

4.2.2 Identification

Several methods have been developed for the identification step, which all rely on using a number of discriminating variables for the separation of fake tau-jets from actual tau-jets. For early data-taking it is foreseen to use a simple cut-based selection using a few robust variables which can be expected to be well-understood at a relatively early stage. Once a better understanding of the whole detector's performance is achieved, more variables can reliably be used, and more complex methods applied for the identification. One of these, which has been used in most simulation studies not concerning early data, is based on the construction of a log-likelihood discriminant. Paper II deals with studies related to this method, which is therefore briefly described in the following.

4.2.2.1 The Log-Likelihood Discriminant Method

The likelihood discriminant is constructed as follows:

$$d = \frac{\mathscr{L}_S}{\mathscr{L}_B + \mathscr{L}_S} \tag{4.1}$$

with $\mathscr{L}_S$ ($\mathscr{L}_B$) being the likelihood that a tau candidate is a real (fake) tau, which can be written as (neglecting correlations between the different input variables):

$$\mathscr{L}_{S(B)} = \prod_{i=1}^{nVars} p_i^{S(B)}(x_i) \tag{4.2}$$

where $p_i^S(x_i)$ ($p_i^B(x_i)$) is the signal (background) probability density function (PDF) for each variable x_i. These distributions are extracted from MC simulation of events containing tau leptons (QCD jets). The variables used depend on the algorithm that reconstructed the tau candidate in question, and whether it is a 1-prong or a 3-prong candidate. Furthermore, the distributions of the variables for 1-prong candidates are considered separately for taus with associated π^0 clusters from those without such clusters.

As the discriminant distribution displays very sharp peaks at 0 and 1, the transformed discriminant d' is used:

$$d' = -\ln\left(\frac{1}{d} - 1\right) = \sum_{i=1}^{i=nVars} \ln \frac{p_i^S(x_i)}{p_i^B(x_i)} \tag{4.3}$$

The distribution of d', which constitutes the output of the log-likelihood method, is shown on the top plot of Figure 4.1. Taus from $Z^0 \rightarrow \tau\tau$ events were used as the signal and jets from QCD dijet events as the background. The right-hand side plot shows the τ efficiency versus the QCD jet rejection, using the same samples. Plots like these are very useful for understanding and comparing the performance of identification methods.

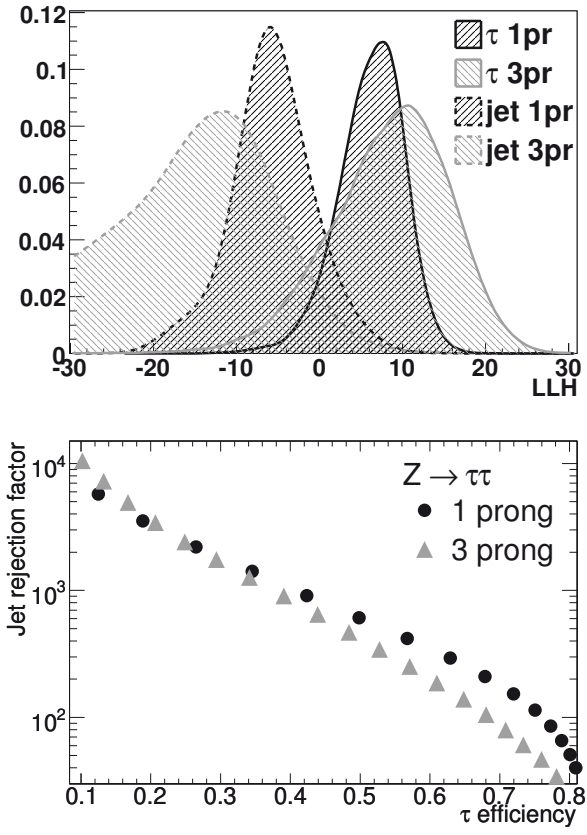

Figure 4.1: Top: Distribution of the tau log-likelihood discriminant output for signal (simulated $Z^0 \rightarrow \tau\tau$ events) and background (simulated QCD dijets), by tau-prong, normalized to unit area. Bottom: τ efficiency versus QCD jet rejection for 1 and 3-prong taus. It should be noted that the distributions depend strongly on the type of events investigated.

5. Summary of Papers

Paper I

This paper presents the measurement of the Lorentz angle in the ATLAS Semi-Conductor Tracker (SCT) using cosmic-ray data collected in 2008. The paper also includes studies of the cluster sizes. The Lorentz angle and the cluster sizes are important observables for studying several aspects of the detector itself. The Lorentz angle is measured by determining the angle of incidence to the silicon wafer, in a plane approximately perpendicular to the magnetic field, corresponding to the minimum average cluster width. In the presence of a magnetic field, this angle equals the Lorentz angle. Several sources of systematics are investigated and accounted for. The Lorentz angle in the SCT barrel, for a temperature of 278.15 ± 1.1 K, a bias voltage of 150 V, and a 2 T magnetic field, is measured as $\theta_L = 3.93 \pm 0.03(stat) \pm 0.10(syst)$, in agreement with the model prediction, $\theta_L = 3.69 \pm 0.26(syst)$. Part of this work will appear in the publication *The ATLAS Inner Detector commissioning and calibration*, currently in preparation and signed by the ATLAS collaboration.

I performed all of the analysis described in this paper, as well as writing substantial parts of the text.

Paper II

This paper presents a study of the identification of tau-jets in two high-multiplicity environments, pile-up and $t\bar{t} \rightarrow \tau$+jets events, in ATLAS. The performance of the log-likelihood discriminant method is known to decrease in such environments, as it was developed with low-multiplicity events (such as $W^{\pm} \rightarrow \tau\nu$) in mind. Several ways to improve the performance as well as the method's robustness were studied. It is shown that using dedicated probability density functions obtained from high-multiplicity events leads to only very marginal improvement. The relative contribution of each discriminating variable is investigated and it is shown that QCD jet rejection can be substantially increased (by more than 50% in some cases) if the worst-performing variables are dropped from the calculation. A number of new variables are also examined and it is shown that some of them outperform existing variables. It is shown that a likelihood containing fewer variables than the currently implemented one would perform better for high-multiplicity environments.

Both authors of this paper thoroughly discussed all parts of the work described and contributed equally to all aspects of this note.

Paper III

This work is a chapter in a much larger publication, which details the expected performance of the ATLAS experiment. This chapter presents the ATLAS senstivity to charged Higgs bosons in five different final states. It is shown that a $H^{\pm}$ could be discovered in a significant fraction of the $(\tan\beta, m_{H^{\pm}})$ parameter space, particularly if it is light, with the region around $\tan\beta = 7$ being the hardest to reach. On the other hand, the exclusion potential for a $H^{\pm}$ lighter than the top quark extends over almost the entire parameter space.

I was responsible for the analysis of the $t\bar{t} \to bH^{\pm}bqq, H^{\pm} \to \tau_{had}\nu$ channel (for $m_{H^{\pm}} < m_t$). This was the first study of this channel using a full simulation of the ATLAS detector, including all trigger levels as well as taking all dominant systematic effects into consideration. A complete rehaul of the previous analysis was necessary, replacing several cuts and introducing a likelihood discriminant in order to suppress the $t\bar{t}$ background. This channel turned out to be the one contributing the most to the expected ATLAS sensitivity to $H^{\pm}$ lighter than the top quark. I was also responsible for the development and maintenance of common $H^{\pm}$ software tools used for most of the channels.

Paper IV

This paper presents a study of heavy charged and neutral Higgs bosons, pair-produced in e^+e^- collisions with a centre-of-mass energy of 3 TeV at the proposed future Compact Linear Collider (CLIC), using a fast detector simulation. High-energy beam-beam effects at the interaction point are taken into account, and their effect on the production cross-section is investigated. It is shown that A^0, H^0 and $H^{\pm}$ could be observed for masses up to and beyond 1 TeV, in the absence of light supersymmetric particles, for an integrated luminosity of 3000 fb^{-1}. It is also shown that the mass of the Higgs bosons can be extracted with a (statistical) error of less than 1% for the same integrated luminosity. Finally it is demonstrated that the $\tan\beta$ parameter can be extracted by comparing signal rates of different decay channels, and that the highest accuracy for such a measurement would be achievable in the region around $\tan\beta = 7$.

I performed most of the analysis presented in this note, as well as implementing the effects of the modified energy spectrum due to beam-beam effects on the background processes.

6. Conclusions

The focus of this thesis is on charged Higgs bosons in the ATLAS experiment and beyond. Charged Higgs bosons are of great interest because their discovery would be a clear signal of non-Standard Model physics, while at the same time furthering our understanding of the Higgs sector. Supersymmetry is one of the most popular theories for physics beyond the Standard Model, and investigations of charged Higgs boson discovery potential are commonly done in the framework of the Minimal Supersymmetric Extension of the Standard Model (MSSM), which requires their presence.

The $t\bar{t} \to bH^{\pm}bqq$, $H^{\pm} \to \tau_{had}\nu$ channel for a $H^{\pm}$ lighter than the top quark was investigated in the context of this thesis, using a detailed simulation of the ATLAS detector, including all trigger levels and considering all dominant systematic effects. It was shown that a discovery should be possible for $\tan\beta$ greater than approximately 20 and for masses up to about 160 GeV, while exclusion should be possible over most of the $(\tan\beta, m_{H^{\pm}})$ parameter space. The study was included in an ATLAS-wide publication of the experiment's expected performance [43], the relevant chapter of which constitutes Paper III. The channel investigated for this thesis is the one contributing most to the combined ATLAS sensitivity for a light $H^{\pm}$.

A charged Higgs boson lighter than the top quark decays predominantly to a τ and a neutrino. As the hadronic τ decay is the most common, a high sensitivity to charged Higgs bosons demands a well-performing reconstruction and identification of tau-jets. Part of the effort for this thesis has therefore been dedicated to refining this aspect of the ATLAS event reconstruction, and more specifically the τ identification using the log-likelihood method in high-multiplicity environments such as pile-up or $t\bar{t}$ events. This is of particular interest for $H^{\pm}$ searches, which operate in such environments, where the performance is known to be worse, as the tau-jet identification has mostly been geared towards low-multiplicity events (*e.g.* $Z^0 \to \tau\tau$ without pile-up). It was shown that although using dedicated probability density functions obtained from high-multiplicity events does not improve the performance much, it is still possible to increase the QCD jet rejection (by more than 50% in certain cases) by dropping a number of variables used in the default method and introducing new ones. This work is documented in Paper II.

Efficient τ reconstruction, like the reconstruction of most other physics objects, depends on efficient tracking and a well-functioning Inner Detector. Part of the work for this thesis has been devoted to the commissioning of the AT-

LAS Semi-Conductor Tracker (SCT), in particular through the measurement of the SCT Lorentz angle using cosmic-ray data collected in the fall of 2008, as detailed in Paper I. The Lorentz angle is an important observable for studying a number of detector aspects, and has to be measured before the detector is irradiated in order to later be able to compare measurements and study the effects of radiation damage. An important part of this work consisted of studying and understanding possible systematic effects. The Lorentz angle in the SCT barrel was measured as $\theta_L = 3.93 \pm 0.03(stat) \pm 0.10(syst)$, in agreement with the model prediction of $\theta_L = 3.69 \pm 0.26(syst)$.

If charged Higgs bosons are discovered at the LHC, measurement of parameters such as mass or $\tan\beta$ will be extremely challenging. Part of the work presented in this thesis, in Paper IV, deals with early studies of the physics potential of a proposed successor to the LHC, the Compact Linear Collider (CLIC) – R&D for which is well underway. It was shown that at CLIC it should, under certain conditions, be possible to measure both the charged Higgs boson mass and $\tan\beta$ with quite high precision. Furthermore, should the charged Higgs boson not be found at the LHC, CLIC should be able to discover it for masses up to 1 TeV or more, depending on the Supersymmetry scenario. The same study also looked at heavy neutral Higgs bosons at CLIC, for which the obtained potential is quite similar.

First collisions have already taken place at the LHC, and soon the first physics results will start appearing. At first, emphasis will lie on completing the commissioning and understanding the detector and its performance. Triggering, reconstruction efficiencies and fake rates, energy scales, and more, all need to be carefully studied and understood before complex analyses such as charged Higgs boson searches can be undertaken. Studies of Standard Model processes will most probably come first, as any search for new physics needs to have its backgrounds under control. Thus, in the context of the charged Higgs boson searches, the weight in the future will lie on developing methods for estimating and extracting from data the background (in particular QCD and $t\bar{t}$), as well as efficiencies for the trigger and the reconstruction. Obtaining a solid handle on these items will be a very important step towards realising the ATLAS detector's potential. Undoubtedly very exciting times lie ahead!

7. Summary in Swedish – Sammanfattning på Svenska

Vad består denna bok du håller i av, rent materiellt? Den består av papper såklart, som i sin tur består av sammanpressade träfibrer. Träfibrerna är uppbygda av molekyler, som i sin tur byggs upp av atomer. Atomerna, vet vi idag, består av en kärna, uppbygd av protoner och neutroner, samt en eller flera *elektroner* (som i en förenklad bild kan ses som svävandes kring kärnan). Protoner och neutroner, slutligen, består av några märkliga partiklar som kallas för *kvarkar*. Så vitt vi vet idag så är elektroner och kvarkar *fundamentala* partiklar, d.v.s. de har inga mindre beståndsdelar[1].

Elementarpartikelfysik är den vetenskap som undersöker dessa materiens minsta beståndsdelar och deras växelverkningar med varandra.

Standardmodellen m.m.

Det vi vet idag om de fundamentala partiklarna beskrivs av en teori som kallas för Standardmodellen. Enligt denna så finns det tre s.k. *generationer* av materiepartiklar, där de två kvarkarna som bygger upp neutroner och protoner, samt elektronen och en partikel som kallas för *elektron-neutrinon* utgör den första generationen. De två andra generationerna består utav tyngre "släktingar" till dessa. Elektonen, elektron-neutrinon, samt deras tyngre släktingar, myonen, tauonen och deras neutriner, kallas för *leptoner*. Allt detta sammanfattas i Tabell 7.1.

Förutom materia förutsäger Standardmodellen även existensen av *antimateria*, dvs (anti)partiklar med samma egenskaper som de materiepartiklar som återfinns i Tabell 7.1 bara det att de har motsatta laddningar (t.ex.elektronens antipartikel, som kallas positron, har positiv laddning). Om en partikel och dess antipartikel förs samman så *annihileras* de och det frigörs energi, ur vilken nya partiklar kan skapas.

I fysiken känner vi till fyra krafter: den elektromagnetiska kraften, gravitationen, den s.k. svaga kraften och den starka kraften. Den elektromagnetiska kraften binder bl.a. elektronerna till atomkärnan, styr alla kemiska processer och ger förstås upphov till alla makroskopiska elektromagnetiska fenomen, som t.ex. färger. Gravitationen är den välbekanta tyngdkraften som gör att massor attraheras till varandra, och den beskrivs av Einsteins allmänna rel-

[1] Det har man förstås trott tidigare också... Ordet "atom" kommer från grekiskans ἄτομον som betyder "odelbar".

Table 7.1: *Kvarkar och leptoner: All i dag känd materia (och antimateria) består i grund och botten utav dessa partiklar (och deras antipartiklar).*

Generation	Kvarkar	Leptoner
I	upp (u), ner (d)	elektron (e^-), elektron-neutrino (ν_e)
II	charm (c), sär (s)	myon (μ^-), myon-neutrino (ν_μ)
III	topp (t), botten (b)	tauon (τ^-), tauon-neutrino (ν_τ)

ativitetsteori. Den svaga kraften är ansvarig för radioaktiva sönderfall och den starka kraften binder samman neutroner och protoner i atomkärnan, samt kvarkarna inuti dessa. Standardmodellen beskriver alla dessa krafter förutom gravitationen, ett problem som vi kommer att återkomma till. Krafterna, även kallade *växelverkningar*, förmedlas enligt Standardmodellen av speciella kraftpartiklar, kallade *bosoner*. Elektromagnetismens boson är *fotonen* (ljuspartikeln), den starka kraftens bosoner kallas *gluoner*, medan den svaga växelverkans bosoner har de mindre fantasifulla namnen $W^\pm$ och Z^0.

Alla dessa (anti)kvarkar, (anti)leptoner och bosoner som beskrivits har man också hittat experimentellt, och alla Standardmodellens förutsägelser har man kunnat experimentellt verifiera – utom en. Det saknas nämligen en partikel, den s.k. *Higgsbosonen*. Enligt Standardmodellen är Higgsbosonen den partikel som ansvarar för att alla andra partiklar ska ha en massa. Utan Higgsbosonen är alla andra partiklar nämligen utan massa. Detta kan vara lite svårt att föreställa sig, men man kan se det som att Higgsbosonen genom sin närvaro kan förändra rummet så att när andra partiklar passerar genom det så får de massa. Problemet är alltså att denna Higgsboson inte har bekräftats genom experiment – och detta utgör en av de största utmaningarna inom experimentell partikelfysik: att upptäcka Higgsbosonen, eller att bevisa att den inte finns.

En annan stor utmaning inom partikelfysik har att göra med huruvida det finns någon fysik "bortom Standardmodellen", som man brukar säga, dvs "ny" partikelfysik som inte innefattas av Standardmodellen. Som redan nämnts beskriver den inte gravitation, och det uppstår problem när man börjar fundera på Higgsbosonens egna massa i samband med detta. Dessutom så beskriver Standardmodellen t.ex. inte heller den "mörka materia" man har observerat i kosmos och som vi inte vet någonting om – den "vanliga" materia som Standardmodellen beskriver, beräknas utgöra endast ynka 4% av universum! Dessa och ytterligare andra tillkortakommanden har lett till att det postulerats ett stort antal teorier som utvidgar Standardmodellen för att lösa dess problem. Den mest dominerande av dessa är Supersymmetri där man lyckas lösa Standardmodellens problem genom att introducera nya s.k. "supersymmetriska partners" till alla Standardmodellens partiklar. Ett intressant resultat av detta är att det krävs inte mindre än fem Higgsbosoner för att ge alla partiklarna

sin massa (man brukar tala om en *Higgssektor* bestående av dessa fem Higgsbosoner). Av dessa fem är två laddade, och det är dessa laddade Higgsbosoner som utgör denna avhandlings primära fokus. Skulle man kunna hitta en laddad Higgsboson skulle detta inte bara kasta ljus på Higgssektorn utan även vara en entydig signal för ny fysik bortom Standardmodellen.

LHC och ATLAS

För att hitta Higgsbosonen, laddad eller ej, eller annan ny fysik, bygger man gigantiska partikelkolliderare, där man accelererar partiklar upp till hastigheter mycket nära ljushastigheten och sedan låter man dem krocka med varandra. I de höga energier som frigörs vid kollisionen kan det skapas nya partiklar och intressanta fenomen kan äga rum. Genom att analysera resultaten av kollisionerna kan man dra slutsatser om vad som hände precis vid krocken och på så vis undersöka om man kanske har sett en helt ny partikel eller ett nytt fenomen.

Den kraftigaste acceleratorn idag är LHC (Large Hadron Collider) som just har startats upp. Den finns i en cirkulär tunnel med 27 km omkrets, vid forskningslaboratoriet CERN, nära Geneve. Två protonstrålar kolliderar vid fyra punkter runt om i tunnelringen och kring dessa kollisionspunkter har man byggt stora detektorer för att studera kollisionerna och de partiklar som kommer ut ur dem. Den största av dessa är ATLAS som är cylindrisk med en längd på cirka 46 m, en diameter på cirka 25 m och en vikt på omkring 7000 ton. ATLAS består av flera detektionslager kring kollisionspunkten. Varje lager är optimerat för att mäta en speciell egenskap eller speciell sorts partikel. Genom att kombinera information från de olika lagren kan man förstå vilken typ av partiklar som kommit ut från kollisionen.

Då LHC precis är i uppstartsfasen så pågår det mycket arbete med att se till att alla detektorer fungerar som de ska, att de är korrekt kalibrerade osv. Den första vetenskapliga artikeln i denna avhandling beskriver ett led i detta arbete, för ett av dessa lager – mätningen av den s.k. Lorentzvinkeln i ATLAS Semi-Conductor Tracker (SCT), en kiselbaserad spårdetektor. När en laddad partikel färdas genom ett magnetfält så känner den av en kraft (Lorentzkraften) i vinkelrät riktning mot såväl magnetfältets riktning som sin egna färdriktning. Då hela spårdetektorn befinner sig i ett starkt magnetiskt fält så påverkar Lorentzkraften laddningsbärarna inne i detektorns aktiva halvledarmaterial: i avsaknad av magnetfält skulle dessa färdas vinkelrätt mot detektorns yta – istället så färdas de i en vinkel p.g.a. Lorentzkraften, och denna vinkel kallas för Lorentzvinkeln. Strömmen från dessa laddningsbärare är det man mäter för att se om en partikel har passerat detektorn, alltså är det viktigt att veta hur stor Lorentzvinkeln är så att man kan kompensera för den i sina mätningar. Dessutom är Lorentzvinkeln intressant att studera för att dra slutsatser om andra aspekter av hur detektorn fungerar. I Artikel I har denna vinkel mätts genom att studera kosmisk strålning som passerat genom och detekterats i ATLAS.

Laddade Higgsbosoner i ATLAS

Genom att datorsimulera kollisionerna och detektorns utslag kan man förbereda analysmetoder för att sedan tillämpa dem på riktig data, eller undersöka om ett fenomen eller en partikel överhuvud taget går att detektera. Inför LHC och ATLAS start har man gjort sådana simuleringsstudier för att utvärdera detektorns förväntade potential när det kommer till mätningar och nya upptäckter. Artikel III är ett kapitel ur en detaljerad sådan studie som gjorts för ATLAS för en mängd fysikprocesser. Detta kapitel handlar om laddade Higgsbosoner och mitt bidrag har i huvudsak varit utförandet av analysen för en av de undersökta sönderfallskedjorna, även kallade *kanaler*. "Min" kanal innehåller en laddad Higgsboson som producerats i sönderfallet av en toppkvark. Hela kanalen jag har studerat kan detaljerat skrivas så här: $t\bar{t} \rightarrow bH^{\pm}bqq$, $H^{\pm} \rightarrow \tau_{had}\nu$, vilket betyder att tillsammans med några andra partiklar så har en laddad Higgsboson skapats och sedan sönderfallit till en tauon-neutino och en tauon; tauonen har sedan haft ett s.k. *hadroniskt* sönderfall (vilket diskuteras senare i denna sammanfattning). Jag har utformat en analysmetod för den och sedan utvärderat ATLAS möjligheter att finna en laddad Higgsboson genom denna kanal. Det visade sig att denna kanal är den mest lovande av alla, ifall laddade Higgsbosoner har en massa som är lägre än toppkvarkens.

Ifall laddade Higgsbosoner existerar, sönderfaller de med största sannolikhet till en tauon-neutrino och en tauon. Detta eftersom Higgsbosoner i allmänhet, enligt de teorier vi har, allra helst sönderfaller till tunga partiklar – och tauonen är den tyngsta av alla leptoner. En tauon är inte en stabil partikel, utan sönderfaller i sin tur också, antingen till lättare leptoner, eller till kvarkar som slår ihop sig till andra partiklar, oftast s.k. *pioner*. Detta sistnämnda sönderfall kallas för hadroniskt, och är det tauon-sönderfall som jag har studerat i denna avhandling. Då en laddad Higgsboson förväntas sönderfalla innan den når ens de innersta lagren av detektorn, så måste man alltså istället detektera tauonen och genom att studera den och de andra partiklarna som skapats, sluta sig till om man ursprungligen haft en laddad Higgsboson som sedan sönderfallit eller inte. Ur en experimentalists synvinkel är det därför mycket viktigt att man kan detektera tauoner på ett bra sätt och att man kan urskilja dem från annat som kanske kan se ut som tauoner vid första anblick. Detta sistnämnda kallas för *identifieringen*, och är en ganska svår process då t.ex. kvarkar kan skapas på många andra sätt än genom en tauons hadroniska sönderfall och kan då i vissa fall ge mycket lika utslag i detektorn. När man utvecklade identifieringsalgoritmen hade man för att utveckla sin metod huvudsakligen använt sig av processer där det enbart skapades tauoner. Detta innebär att om man skulle använda metoden på processer, som t.ex. den kanal jag studerat, där tauonen skapas tillsammans med många andra partiklar, så fungerar den inte lika bra. I Artikel II har vi undersökt detta och försökt hitta sätt att förbättra metoden i sådana sammanhang. Genom att plocka bort variabler som inte

bidrog, samt lägga till en del nya, lyckades vi få metoden att bättre urskilja felaktiga tauon-kandidater.

Efter LHC?

Det kanske låter konstigt att man redan funderar på vad som händer efter LHC, när denna maskin knappt har startat. Dock så är det så med dessa gigantiska projekt vi har i elementarpartikelfysik att tiden det tar att utveckla nästa generations anläggning är så lång att man måste börja med dess utväckling innan den nuvarande ens kommit igång. En föreslagen efterföljare till LHC heter CLIC (Compact Linear Collider) som, till skillnad från LHC som är cirkulär och kolliderar protoner, föreslås vara linjär och kollidera elektroner och positroner. Det pågår redan mycket forskning kring CLIC och då är det förstås också intressant att veta vad man skulle kunna åstadkomma med en sådan maskin, i termer av upptäckter och mätningar. Det första steget är att göra simuleringsstudier, vilket gjorts i Artikel IV för både laddade och tunga neutrala Higgsbosoner. Om man inte skulle kunna upptäcka sådana med LHC, visar vi att man har en riktigt god chans att hitta dem med CLIC. Och även om man skulle upptäcka dem med LHC så skulle det vara mycket svårt att mäta vissa intressanta parameterar, som t.ex. deras massa. Vid CLIC skulle man under de rätta omständigheterna kunna mäta dessa parametrar med stor noggranhet.

Spännande tider

Detta är onekligen en mycket spännande tid att forska inom partikelfysik. Mycket fokus ligger just nu på LHC. Det är inte bara partikelfysiker som tycker att dess uppstart är spännande, även allmänheten och media har visat stort intresse. Första kollisionerna har redan skett, energin i strålarna ska succesivt skruvas upp för att nå nya, aldrig tidigare uppnådda nivåer, och snart kommer de första fysikmätningarna att presenteras. Mycket arbete kommer att krävas för att få allt att fungera som det ska, men när allt är på plats så kan vi börja söka efter tecken från Higgsbosoner, Supersymmetri och en massa andra terorier – men ingen vet vad vi kommer att finna. Vi träder in i helt outforskade fysikområden och det vi hittar kanske inte alls stämmer överens med någon av de teorier vi på förhand byggt upp – och det är ju det som är mest spännande!

Acknowledgements

A large number of people are to be thanked for directly or indirectly assisting me during my doctoral studies. I start by thanking Richard Brenner, my advisor, for our open communication; for all the advice and help on a great number of issues both in physics and of a more practical nature; for many interesting discussions on a large variety of topics, from finnish-swedish vocabulary to the merits of crème brûlée – and also for introducing me to squash. I also wish to thank my co-advisor and group leader, Tord Ekelöf, for all support and advice, as well as for a number of very enjoyable dinners. I am very grateful to both you and Richard for providing favourable working conditions and all the needed infrastructure in the Uppsala ATLAS group, allowing me to work independently and take on responsibilities within the ATLAS collaboration.

During my first steps as a PhD-student I profited immensely from the experience, competence and friendly manner of Bjarte Mohn. In addition to a lot of valuable help with physics analysis, you introduced me to, and guided me through, the mysteries of the ATLAS software, as well as many of the intricacies of working within such a huge collaboration.

My doctoral studies would have been very different without my fellow PhD-student and good friend Martin Flechl. We worked together on many of our projects and it has been both a pleasure and a privilege, which I hope will continue also after our time in Uppsala. I have learnt a lot from our collaboration, not the least about mailing-list netiquette! Your superior knowledge of linux has, on numerous occasions, been invaluable – as have your accute observations on everything between likelihood distributions and football results.

Oscar Stål has been a good friend since our common undergraduate studies, and having you around has been a great resource. I have always valued and enjoyed our discussions, which have shed clarity on many topics in physics (and beyond!). I hope and believe that we will keep them up also in the future!

Camille Bélanger-Champagne has contributed a lot with her intelligence and pleasant manner on both the academic and social plane. I have much enjoyed our conversations – I only wish I had been as good at exercising and improving my French as you your Swedish!

Arnaud Ferrari is the person who introduced me to particle physics, supervising my master thesis. For this and for all subsequent advice I am thankful, as I am for getting such a good master thesis topic that it eventually led to a journal publication. But more than that, I am thankful for your great company and your relaxed attitude – even if you make us all jealous with your travels!

Johan Rathsman has always been a person I have felt I can talk to, and he has generously provided assistance on many topics, helpfully explaining difficult concepts. Similarly, I have on a number of occasions benefitted from the advice of Gunnar Ingelman. The two of them as well as David Eriksson, Johan Alwall, Nazila Mahmoudi and other members of the THEP group deserve my gratitude for freely sharing their expertise on both theory and other matters, as well as for being very pleasant people to have around!

Mattias Ellert deserves many thanks for all the assistance on a great variety of technical issues, and his helpful attitude no matter how stupid my question.

Claus Buszello has always shown an interest in my work and often provided good suggestions and ideas, typically over a lunch at R2!

I have also profitted from the advice, help and support of many ATLAS people outside of Uppsala University, such as Kétévi Assamagan, Steve McMahon, Reisaburo Tanaka, Pat Ward and many more, and I thank them all.

I am particularly grateful to Inger Ericson for making difficult problems simple, and simple problems disappear, while always being pleasant. You are also the reason I do not take my coffee with sugar any more!

Magnus, we have had many good times together, and I have often missed your skånska at the department! Karin and Peder, I very much appreciated our lunches at Rullan. P-A, the strongest follower of the Thursday beer! Agnes, Anni, Annica, Bengt, Charlie, Emma, Erik, Henrik, Henrik, Karin, Kristoffer, Markus, Martin, Mikael, Olle, Patrik, Rikard, Sophie, Stephan, Volker, Örjan, and many other people at the department should be thanked for providing good company during lunches, coffee-breaks, Christmas parties and more.

During my year at CERN I met a lot of fun, welcoming people who I wish to thank for all the good times that have been, and that will come! Special mention to Christian and Seth, who had to live with a practically absent flatmate, too busy working for this thesis.

Stefan – I have very much appreciated the ACBs, as well as your "technical assistance" in the final phases of this thesis.

I also want to thank all my friends outside physics, who mysteriously still like to spend time with me, even if I often talk about incomprehensible things, work late hours and am always busy. Special mention to Yiannis, Erik and everybody in DGJ and in "the Rome group", Dimitris, Johan, Axel, Johan, Erik, as well as all the great people I met during my time in BEST.

I am very grateful to Ritos and Fragoula who always helped me with many practical things, in particular when I had just arrived in Uppsala.

Very special thanks to Rebeca. Remember, 0-1 or as much as 2!

A great thank-you to all the people who read and commented on the manuscripts to this thesis: Richard, Martin, Enzo, Oscar and Johan.

Finally, I want to thank my family. Amanda for being my best sister in the world; Thomas and Lotta for having done so many things for me that it does not make sense to enumerate them. Tack! Ευχαριστώ!

Bibliography

[1] *LHC Yellow Book*. CERN, 1995. CERN-AC-95-05.

[2] P. Higgs, *Broken Symmetries and the Mass of the Gauge Bosons*, *Phys. Rev. Lett.* **13** (1964) 508–509.

[3] P. Higgs, *Broken symmetries, massless particles and gauge fields*, *Phys. Lett.* **12** (1964) 132–133.

[4] **ATLAS** Collaboration, G. Aad *et. al.*, *The ATLAS Experiment at the CERN Large Hadron Collider*, *JINST* **3** (2008) S08003.

[5] R. W. Assmann *et. al.*, *A 3 TeV e^+e^- Linear Collider Based on CLIC Technology*. CERN, Geneva, 2000. CERN 2000-008.

[6] S.L.Glashow, *Partial symmetries of weak interactions*, *Nucl.Phys.* **22** (1961) 579–588.

[7] S.Weinberg, *A model of leptons*, *Phys.Rev.Lett.* **19** (1967) 1264–1266.

[8] A.Salam, *Weak and electromagnetic interactions*, in *Elementary Particle Theory, Proceedings of the Nobel Symposium held 1968 at Lerum, Sweden* (N.Svartholm, ed.), pp. 367–377. Almqvist & Wiksell, 1968.

[9] **LEP Working Group for Higgs boson searches** Collaboration, R. Barate *et. al.*, *Search for the standard model Higgs boson at LEP*, *Phys. Lett.* **B565** (2003) 61–75, [hep-ex/0306033].

[10] **SNO** Collaboration, Q. R. Ahmad *et. al.*, *Measurement of the charged current interactions produced by B-8 solar neutrinos at the Sudbury Neutrino Observatory*, *Phys. Rev. Lett.* **87** (2001) 071301, [nucl-ex/0106015].

[11] P. Ramond, *The Family Group in Grand Unified Theories*, hep-ph/9809459.

[12] **WMAP** Collaboration, C. L. Bennett *et. al.*, *First Year Wilkinson Microwave Anisotropy Probe (WMAP) Observations: Preliminary Maps and Basic Results*, *Astrophys. J. Suppl.* **148** (2003) 1, [astro-ph/0302207].

[13] K. D. Lane, *Technicolor 2000*, hep-ph/0007304.

[14] M. Schmaltz and D. Tucker-Smith, *Little Higgs Review*, *Ann. Rev. Nucl. Part. Sci.* **55** (2005) 229–270, [hep-ph/0502182].

[15] M. Shifman, *Large Extra Dimensions: Becoming acquainted with an alternative paradigm*, arXiv:0907.3074.

[16] J.Wess and B.Zumino, *Supergauge transformations in four dimensions*, *Nucl.Phys.* **B70** (1974) 39–50.

[17] P. Binetruy, *Supersymmetry: Theory, Experiment, and Cosmology*. 2006. Oxford University Press.

[18] S. L. Adler, *Axial-vector vertex in spinor electrodynamics*, *Phys. Rev.* **177** (Jan, 1969) 2426–2438.

[19] J. S. Bell and R. Jackiw, *A PCAC puzzle: pi0 → gamma gamma in the sigma model*, *Nuovo Cim.* **A60** (1969) 47–61.

[20] J.Gunion, H.Haber, G.Kane, and S.Dawson, *The Higgs Hunter's Guide*. Addison-Wesley, Reading, UK, 1990.

[21] J. Alwall and J. Rathsman, *Improved description of charged Higgs boson production at hadron colliders*, *JHEP* **12** (2004) 050, [hep-ph/0409094].

[22] T. Sjöstrand, P. Eden, C. Friberg, L. Lönnblad, G. Miu, S. Mrenna, and E. Norrbin *Comp. Physics Commun.* **135** (2001) 238.

[23] M. Spira, *QCD effects in Higgs physics*, *Fortsch. Phys.* **46** (1998) 203–284, [hep-ph/9705337].

[24] S. Heinemeyer et al., *Feynhiggs version 2.6.2*, 2007. hep-ph/0611326, hep-ph/0212020, hep-ph/9812472, hep-ph/9812320.

[25] **ALEPH, DELPHI, L3 and OPAL** Collaboration, S. Schael *et. al.*, *Search for neutral MSSM Higgs bosons at LEP*, *Eur. Phys. J.* **C47** (2006) 547–587, [hep-ex/0602042].

[26] A. Djouadi, J. Kalinowski, and M. Spira, *HDECAY: A program for Higgs boson decays in the Standard Model and its supersymmetric extension*, *Comput. Phys. Commun.* **108** (1998) 56–74, [hep-ph/9704448].

[27] The TEVNPH Working Group for the CDF and D0 Collaborations, *Combined CDF and D0 upper limits on MSSM Higgs boson production in tau-tau final states with up to 2.2 fb-1 of data*, FERMILAB-PUB-09-394-E.

[28] **ALEPH** Collaboration, A. Heister *et. al.*, *Search for charged Higgs bosons in e^+e^- collisions at energies up to $\sqrt{s}$ = 209-GeV*, *Phys. Lett.* **B543** (2002) 1–13, [hep-ex/0207054].

[29] **CDF** Collaboration, A. Abulencia *et. al.*, *Search for charged Higgs bosons from top quark decays in $p\bar{p}$ collisions at $\sqrt{s} = 1.96$-TeV*, *Phys. Rev. Lett.* **96** (2006) 042003, [hep-ex/0510065].

[30] **D0** Collaboration, V. M. Abazov *et. al.*, *Search for charged Higgs bosons in top quark decays*, *Phys. Lett.* **B682** (2009) 278–286, [arXiv:0908.1811].

[31] D. Eriksson, F. Mahmoudi, and O. Stål, *Charged Higgs bosons in Minimal Supersymmetry: Updated constraints and experimental prospects*, *JHEP* **11** (2008) 035, [arXiv:0808.3551].

[32] O. S. Brüning, P. Collier, P. Lebrun, S. Myers, R. Ostojic, J. Poole, and P. Proudlock, *LHC Design Report*. CERN, Geneva, 2004.

[33] **CMS** Collaboration, G. L. Bayatian *et. al.*, *CMS physics: Technical design report*. CERN-LHCC-2006-001.

[34] **LHCb** Collaboration, *LHCb technical design report: Reoptimized detector design and performance*. CERN-LHCC-2003-030.

[35] **ALICE** Collaboration, *ALICE: Technical proposal for a large ion collider experiment at the CERN LHC*. CERN-LHCC-95-71.

[36] https://twiki.cern.ch/twiki/bin/view/Atlas/ApprovedPlotsSCT.

[37] **GEANT4** Collaboration, S. Agostinelli *et. al.*, *GEANT4: A simulation toolkit*, *Nucl. Instrum. Meth.* **A506** (2003) 250–303.

[38] **ILC** Collaboration, J. Brau, (Ed.) *et. al.*, *ILC Reference Design Report Volume 1 - Executive Summary*, arXiv:0712.1950.

[39] F. Tecker. Private Communication.

[40] **CLIC Study Team** Collaboration, H. Braun *et. al.*, *CLIC 2008 parameters*, . CERN-OPEN-2008-021.

[41] R. Appleby, A. Ferrari, M. Salt, and V. Ziemann, *Conceptual design of a beam line for post-collision extraction and diagnostics at the multi-TeV Compact Linear Collider*, *Phys. Rev. ST Accel. Beams* **12** (2009) 021001.

[42] **Particle Data Group** Collaboration, C. Amsler *et. al.*, *Review of particle physics*, *Phys. Lett.* **B667** (2008) 1.

[43] **The ATLAS** Collaboration, G. Aad *et. al.*, *Expected Performance of the ATLAS Experiment - Detector, Trigger and Physics*, arXiv:0901.0512. CERN-OPEN-2008-020.

Acta Universitatis Upsaliensis

Digital Comprehensive Summaries of Uppsala Dissertations from the Faculty of Science and Technology 702

Editor: The Dean of the Faculty of Science and Technology

A doctoral dissertation from the Faculty of Science and Technology, Uppsala University, is usually a summary of a number of papers. A few copies of the complete dissertation are kept at major Swedish research libraries, while the summary alone is distributed internationally through the series Digital Comprehensive Summaries of Uppsala Dissertations from the Faculty of Science and Technology. (Prior to January, 2005, the series was published under the title "Comprehensive Summaries of Uppsala Dissertations from the Faculty of Science and Technology".)

Distribution: publications.uu.se
urn:nbn:se:uu:diva-111576

ACTA
UNIVERSITATIS
UPSALIENSIS
UPPSALA
2010